Theses and Dissertations

Student Graduate Works

9-2006

Parameter Estimation of a Tactical Missile using Linear Regression

Kelly S. Powers

PARAMETER ESTIMATION OF A TACTICAL MISSILE USING

LINEAR REGRESSION

THESIS

Kelly S. Powers

AFIT/GAE/ENY/06-S12

DEPARTMENT OF THE AIR FORCE
AIR UNIVERSITY

AIR FORCE INSTITUTE OF TECHNOLOGY

Wright-Patterson Air Force Base, Ohio

The views expressed in this thesis are those of the author and do not reflect the official policy or position of the United States Air Force, Department of Defense, or the United States Government.

AFIT/GAE/ENY/06-S12

PARAMETER ESTIMATION OF A TACTICAL MISSILE USING LINEAR REGRESSION

THESIS

Presented to the Faculty

Department of Aeronautical and Astronautical Engineering

Graduate School of Engineering and Management

Air Force Institute of Technology

Air University

Air Education and Training Command

In Partial Fulfillment of the Requirements for the

Degree of Master of Science in Aeronautical Engineering

Kelly S. Powers, BS

August 2006

AFIT/GAE/ENY/06-S12

PARAMETER ESTIMATION OF A TACTICAL MISSILE USING LINEAR REGRESSION

Kelly S. Powers, BS

Approved:

_____   28 Aug 06
Dr. David Jacques, Ph.D. (Chairman)   Date

_____   28 Aug., 06
Dr. Meir Pachter, Ph.D. (Member)   Date

_____   28 Aug 06
Paul Blue, Maj, USAF (Member)   Date

AFIT/GAE/ENY/06-S12

Abstract

The purpose of this research was to present the method of Linear Regression as a parameter identification method to determine the longitudinal dimensional stability derivatives of a tactical missile. Missile flight histories are characterized by rapid accelerations, rapidly changing mass property characteristics with often short flight times. These characteristics make accurate parameter estimation of the missile aerodynamics more challenging than for aircraft. The simulation used for this research was created in MATLAB/SIMULINK based on the missile trajectory program, TRAP. The aerodynamic data for the 6-DoF missile model was based on a supersonic, tail controlled missile similar to an AIM-9X missile. Two command input types were investigated to determine if either could induce an excitation of the system modes of the plant being measured to lead to good estimates of the model parameters. These two input types were a high-frequency pitch doublet and band-limited white noise.

The research indicated the conclusion: While the method is not as complex as other parameter estimation methods, this research shows that linear regression can be used successfully in determining longitudinal dimensional stability derivatives of a tactical missile in flight when using a control input form with higher frequency modulations, such as band-limited or filtered white noise.

Table of Contents

List of Figures

List of Tables

PARAMETER ESTIMATION OF A MISSILE USING LINEAR REGRESSION

1. Introduction

1.1 General

Aerodynamic force and moment databases for tactical missile trajectory simulations are usually populated with an evolving mix of analytical and wind tunnel derived aerodynamic predictions. The fidelity of these simulations can be improved by incorporating flight test derived estimates of aerodynamic characteristics. Parameter estimation allows for a better understanding of theoretical predictions, improves wind tunnel databases, aides in the development of flight control systems and provides more accurate representations of the missile in all flight regimes.

The work presented here is concerned with the parameter estimation of a tactical missile utilizing the linear regression, least squares algorithm. While linear regression is widely understood in the scientific and mathematical world, little work has been done in applying the least squares method to predict aerodynamic parameters of tactical missiles.

1.2 Background

Several methods are available for aerodynamic system identification from flight test data. The primary problem is determining which methods are most applicable to tactical missiles. Missile flight histories are characterized by rapid accelerations, rapidly changing weight, inertia and thrust characteristics, and often, short flight times. These characteristics make accurate parameter estimation of missile aerodynamics more challenging than for aircraft.

The concept of aerodynamic parameter determination from flight test data has been successfully applied to aircraft. An aircraft used in flight test applications can be well equipped with complex instrumentation and sensors, which can be utilized repeatedly for numerous tests. Control surface inputs can be designed to intentionally separate complex aerodynamic effects or excite aircraft motion while at a particular flight condition. This allows for the usage of simplified aerodynamic models linearized about a certain flight condition. Flight tests can also be repeated if necessary when sensor or telemetry problems arise. [1]

In contrast, aerodynamic parameter determination from flight test data for a missile flight test program presents a more difficult problem. Because of the cost and the destructive nature of a missile, relatively few flight tests can be afforded. Flight tests that are scheduled usually have other objectives in addition to determining the aerodynamic parameters of the missile. Therefore, the opportunity to set up the missile control surfaces to determine the aerodynamic parameters might not be available. Most missile flights involve large and rapid variations in flight condition. This minimizes the flight regime in which a simplified aerodynamic model will be accurate for the missile flight test. [1] Therefore, multiple aerodynamic models are needed to encompass the missile flight test envelope. This would significantly increase computational time required for the missile parameter estimation technique.

Several methods used for system identification include, Linear Regression (or Least Squares), Maximum Likelihood and Extended Kalman Filters. The Maximum Likelihood estimator method has been successfully used to determine aerodynamic parameters for over 40 years. Most of this work has been done using aircraft and not

much research has been found applying this method to tactical missiles. The Maximum Likelihood method is popular because it can generate statistically optimum estimates of constant parameters.[2] This, however, puts the Maximum Likelihood method at a disadvantage when estimating missile aerodynamic parameters due to the fact that during the missile flight test, large deviations from nominal flight conditions are to be expected. Popular programs that implement the Maximum Likelihood estimator are PEST, MMLE, and PARAIDE.

The Extended Kalman Filter, EKF, method generates statistically minimum variance optimum estimates that can be time-varying and is also considered numerically efficient.[2] This allows the EKF method to be applied to flight test environments in which the system parameters are not held constant. In this method, the system equations are linearized about the state-parameter vector in order to determine the optimal system estimate. The maximum likelihood method avoids the linearization constraints of the EKF method; however, by doing so, it introduces excessive computational burdens and numerical difficulties.

Linear regression has been used recently by the Air Force Research Laboratory for the system identification of on-line reconfigurable flight control. The system identification algorithm studied identified rapid changes in parameters caused by failure and/or damage. Early work developed relationships from flight mechanics to regularize the linear regression estimates. Classical linear regression was augmented to include stochastic constraints, which were used to model uncertainty in the information conveyed by the constraints. In the interest of generality, the a priori estimates of the stability and control derivatives were used instead as regularization constraints, where the variance

represents the uncertainty in the a priori estimates.[3] The methodology was expanded by additional research that entailed a regularization process where the regressor matrix was subjected to a singular value decomposition that led to a reparametrization of the original estimation problem, where information about the parameter vector, conveyed by the data, was extracted. Then, a priori information was used to regularize the estimation problem and obtain an estimate of the original parameter vector.[4] The work was then extended to include over-actuated aircraft, i.e., aircraft with distributed control effectors. This development was demonstrated on the F-16 VISTA aircraft for both the lateral and longitudinal axes. The results of the research showed that even during periods of low excitation, the parameter estimates had been improved by utilizing a priori information.

1.3 Research Objective

The objective of this research is to determine the applicability of using the Linear Regression method to determine the aerodynamic parameters of a highly maneuverable tactical missile. Specifically, the research will determine the longitudinal aerodynamic parameters and compare them to the truth data to determine the viability of the method for use as a parameter identification tool. The research will also determine the best command input form to drive the 6-Degree of Freedom missile simulation that will generate good estimates from the Linear Regression method.

1.4 Approach and Scope

The work here presents the Linear Regression method as a possible tool for parameter identification of a missile. The Linear Regression method was to be applied to real flight test data from a missile after launch. However, data from real flight test experiments was not available for this research, so a 6 Degree-of-Freedom missile simulation in MATLAB/SIMULINK was used to generate a data set representative of data collected from a real flight test. The aerodynamic data for the 6-DoF missile model was based on a supersonic, tail controlled missile with similar geometry and mass properties of an AIM-9X missile. The missile aerodynamics of the model were limited to include only first-order effects due to limitations in the semi-empirical prediction code, Missile DATCOM, utilized for this research. The missile model does not include actuator dynamics, but defines different combinations of individual control surface deflections into net deflections for δP (Roll deflection command), δQ (Pitch deflection command) and δR (Yaw deflection command).

From the data collected, the Linear Regression method was used to determine the three longitudinal dimensional stability derivatives, M_α, M_q and $M_{\delta e}$. The Linear Regression method was validated first using a longitudinal linear model of the system with known parameters. These parameters were then estimated using the Linear Regression method and compared to the known parameters for validation.

The Linear Regression method was then applied to the parameters, α (angle of attack in degrees), q (pitch rate in degrees/sec), δe (Elevator angle in degrees) and

$\overset{.}{q}$ (pitch acceleration in degrees/sec^2) obtained from the 6-DoF simulation data to determine estimates of the longitudinal stability derivatives. The estimates were compared to the truth data from the aerodynamic model of the missile simulation. The Linear Regression was applied once more using a linear model of the system that used the initial estimates obtained from the simulation data as the new truth data. Once again, for validation purposes, the Linear Regression estimates were compared to the earlier estimates from the 6-DoF simulation.

1.5 Relevance

This research is intended to investigate the feasibility of applying Linear Regression techniques to determine aerodynamic coefficients of a missile model. It is not intended to compare results found by using Linear Regression to other well-known parameter identification methods. The intent of this research is to provide useful findings to help improve the fidelity of aerodynamic force and moment databases for tactical missile trajectory simulations.

1.6 Document Overview

The document starts in Chapter 2 with an introduction to Linear Regression and the equations and their derivations that were used in this research. Chapter 3 provides the background needed to understand the missile simulation created in SIMULINK that was used for this research. It includes descriptions of the missile simulation, missile aerodynamics and autopilot that make up the 6-degree-of-freedom simulation. Chapter 4 combines both topics from Chapter 2 and Chapter 3 to produce results and analysis of the

proposed parameter identification method. Chapter 5 goes over conclusions found from

this research and proposes further research to expand on what was learned.

2. Linear Regression Technique

2.1 Overview

The purpose of this chapter is to provide a review of the theory of least squares or Linear Regression, as is described from Reference 5. Least-squares theory has become a major tool for parameter estimation of experimental data. While other estimation methods exist, such as Maximum Likelihood and Extended Kalman filters, the least-squares method continues to be the most understood among engineers and scientists. This is due to the fact that the method is easier to understand than other methods and does not require knowledge of mathematical statistics. The method also may provide solutions in cases where other methods have failed. Estimates obtained by the least-squares method have optimal statistical properties; they are consistent, unbiased and efficient.

2.2 Least-Squares Theory

The least-squares technique provides a mathematical procedure by which a model can achieve a best fit to experimental data in the sense of minimum-error-squares. Suppose there is a variable y that is related linearly to a set of n variables, $x = (x_1, x_2, ..., x_n)$, that is

$$y = \theta_1 x_1 + \theta_2 x_2 + ... + \theta_n x_n \qquad (2.1)$$

where $\theta = (\theta_1, \theta_2, ..., \theta_n)$ is a set of constant parameters. θ are unknown and we wish to estimate their values by observing the variables y and x at different times.

Assuming that a sequence of m observations on both y and x has been made at times

$t_1, t_2, ..., t_m$, we can now relate the data by the following set of m linear equations:

$$y(i) = \theta_1 x_1(i) + \theta_2 x_2(i) + ... + \theta_n x_n(i), i = 1, 2, ..., m \tag{2.2}$$

This equation is called a regression function and θ are the regression coefficients.

This system of equations (2.2) can be arranged into a simple matrix form:

$$y = x\theta \tag{2.3}$$

where,

$$y = \begin{bmatrix} y(1) \\ y(2) \\ y(3) \\ \vdots \\ y(m) \end{bmatrix} \quad X = \begin{bmatrix} x_1(1) & \cdots & x_n(1) \\ x_1(2) & \cdots & x_n(2) \\ \vdots & & \vdots \\ x_1(m) & \cdots & x_n(m) \end{bmatrix} \quad \theta = \begin{bmatrix} \theta_1 \\ \theta_2 \\ \vdots \\ \theta_n \end{bmatrix} \tag{2.4}$$

There are several different instances that can occur when determining the solution of

Equation 2.4 based on the sizes of m and n.

If $m = n$, then we can solve for θ uniquely by

$$\hat{\theta} = X^{-1} y \tag{2.5}$$

provided that X^{-1}, the inverse of the square matrix X, exists. $\hat{\theta}$ denotes the estimate of

θ.

When $m < n$ and $rank(X) = m$, there are an infinite number of solutions, the problem is

under-constrained. In general, this problem has an infinite number of solutions θ which

exactly satisfy $y - X\theta = 0$. In this case it is often useful to find the unique solution for θ

which minimizes $\|\theta\|_2$. This problem is referred to as finding a minimum norm solution to an underdetermined system of linear equations.

In the most usual case, $m > n$ and $rank(X) = n$, there is no solution for $y = X\theta$. The problem is also referred to as finding a least squares solution to an over-determined system of linear equations, where $\hat{\theta}$ is chosen to minimize $\left\| y - X\hat{\theta} \right\|$.

The best approach to solving the over-determined equation (2.5) would be to determine $\hat{\theta}$ on the basis of least-error-squares described in the next section.

2.2.1 Least-Error-Squares

For, $y \notin R(X)$

Define an error vector $e = (e_1, e_2, ..., e_m)^T$ and let

$$e = y - X\theta \tag{2.6}$$

$\hat{\theta}$ will be chosen in such a way to minimize the criterion J

$$J = \sum_{i=1}^{m} e_i^2 = e^T e \tag{2.7}$$

To carry out the minimization, J is expressed as

$$J = (y - X\theta)^T (y - X\theta)$$

$$= y^T y - \theta^T X^T y - y^T X\theta + \theta^T X^T X\theta$$

Differentiating J with respect to θ and equating the result to zero to determine the conditions that the estimate $\hat{\theta}$ minimizes J, provides the necessary condition for the optimal estimate

$$\left.\frac{\partial J}{\partial \theta}\right|_{\theta = \hat{\theta}} = -2X^T y + 2X^T X \hat{\theta} = 0$$

This yields

$$X^T X \hat{\theta} = X^T y \tag{2.8}$$

Solving for $\hat{\theta}$

$$\hat{\theta} = (X^T X)^{-1} X^T y \tag{2.9}$$

Where $(X^T X)^{-1} X^T$ is commonly referred to as the pseudo-inverse.

This result is known as the least-squares estimator (LSE) of θ, also called ordinary least squares.

2.3 Statistical Properties of Least-squares Estimators

In this section the statistical qualities of the least-squares estimators are examined. Looking at Equation (2.6), where the vector e can be thought of as the measurement noise and or modeling error, the noise-disturbed system equation is

$$y = X\theta + e \tag{2.10}$$

It is assumed that e is a stationary random vector with zero mean value, $E[e] = 0$ and that e is uncorrelated with y and X, i.e. white noise. Based on these assumptions about e, it is possible to determine the accuracy of the parameter estimates given by equation (2.9).

In general, $\hat{\theta}$ is a random variable. The accuracy can be measured by a number of statistical properties such as bias, error covariance, efficiency and consistency. These terms will be defined later in the chapter.

22

First showing that $\hat{\theta}$ is unbiased, meaning that $E\left[\hat{\theta}\right] = \theta$. Substituting equation (2.10)

into (2.9), becomes

$$\hat{\theta} = \theta + (X^T X)^{-1} X^T e \tag{2.11}$$

Taking the expectation on both sides of equation (2.11) and applying the

property $E[e] = 0$, the desired result is obtained, proving that $\hat{\theta}$ is unbiased.

$$E\left[\hat{\theta}\right] = E[\theta] + E\left[(X^T X)^{-1} X^T\right] E[e] = \theta \tag{2.12}$$

The covariance matrix corresponding to the estimate error $\hat{\theta} - \theta$ is

$$\Psi \overset{\Delta}{=} E\{(\hat{\theta} - \theta)(\hat{\theta} - \theta)^T\}$$

$$= E\{[(X^T X)^{-1} X^T e][(X^T X)^{-1} X^T e]^T\}$$

$$= (X^T X)^{-1} X^T E\{ee^T\} X (X^T X)^{-1}$$

Define the covariance matrix of the error vector e to be

$$R = E[ee^T] \tag{2.13}$$

Ψ is reduce to

$$\Psi = (X^T X)^{-1} X^T R X (X^T X)^{-1} \tag{2.14}$$

When the noise $e(i), i = 1,2,...,$ are identically distributed and independent with zero

mean and variance σ^2, the covariance R becomes

$$R = E[ee^T] = \sigma^2 I \tag{2.15}$$

23

This implies that the corresponding LSE $\hat{\theta}$ is a minimum variance estimator. $\hat{\theta}$ is called an efficient estimator.

Lastly, LSE $\hat{\theta}$ will be shown as a consistent estimator. Rewriting the error covariance matrix Ψ in the form of

$$\Psi = \sigma^2 (X^T X)^{-1} = \frac{\sigma^2}{m}\left(\frac{1}{m} X^T X\right)^{-1} \tag{2.16}$$

where $R = \sigma^2 I$ is assumed and in which m is the number of equations in the vector equation (2.10). Assume that $\lim_{m\to\infty}[(1/m)X^T X]^{-1} = \Gamma$, where Γ is a nonsingular constant matrix. Then

$$\lim_{m\to\infty} \Psi = \lim_{m\to\infty} \frac{\sigma^2}{m}\left(\frac{1}{m} X^T X\right)^{-1} = 0 \tag{2.17}$$

Zero error covariance means that $\hat{\theta} = \theta$ at $m \to \infty$. This convergence property indicates that $\hat{\theta}$ is a consistent estimator.

It has been shown in this section that the LSE in the presence of white noise is unbiased, efficient, and consistent, therefore the least squares technique does have many advantages. The method described in this chapter will be applied to results obtained from the 6-degree-of-Freedom missile simulation described in the next chapter, Chapter 3.

3. Missile Model and Simulation Environment

3.1 Overview

This chapter presents the missile simulation that will be used to generate

simulation data that the Linear Regression technique, described in Chapter 2, will employ

for parameter identification. The missile was modeled as a six-degree-of-freedom

SIMULINK model within a 1 vs. 0 simulation developed by the Air-to-Air Weapons

Branch, Aircraft and Electronics Division, National Air and Space Intelligence Center

(ADNW/NASIC). This simulation is currently used to determine missile capabilities and

to demonstrate those capabilities in enemy engagement scenarios. This section discusses

the missile data and the simulation obtained from ADNW/NASIC and changes that were

made to facilitate this research.

This chapter lays out the background needed to understand the Missile simulation created

in SIMULINK that was used for this research. Section 3.1 describes the framework,

components and environments in the missile engagement simulation. Section 3.2

describes the aerodynamic model of the missile first by defining the aerodynamic angle

and control surface deflection conventions. The aerodynamic coefficients and forces and

moment equations are then presented leading up to finally reach the Translational and

Rotational Equations of motion for the missile airframe. Section 3.2 ends with a

description of the type of missile used for the research and how the aerodynamic data was

generated for the model. Section 3.3 describes the acceleration- controlled autopilot used

to control the missile model.

3.2 Missile Simulation

The simulation used for this research was modified from an existing simulation developed by NASIC/ADNW in MATLAB/SIMULINK that was based on the missile trajectory program, TRAP (TRajectory Analysis Program). The simulation represented a 1 vs. 0 engagement with an air-to-air missile fire.

3.2.1 Simulation Components

The simulation is setup to simulate three vehicles: a launch aircraft, a missile and a target aircraft. It is built around a detailed fly-out model for the missile with simplified launch aircraft and target models. The launch aircraft is modeled as a pseudo 5-degree of freedom, or modified point-mass model. The target aircraft is a 3 degree of freedom or point-mass model and the missile is a 6 degree of freedom model. All three models in the simulation were modeled having Flat-Earth kinematics. A typical engagement is illustrated below.
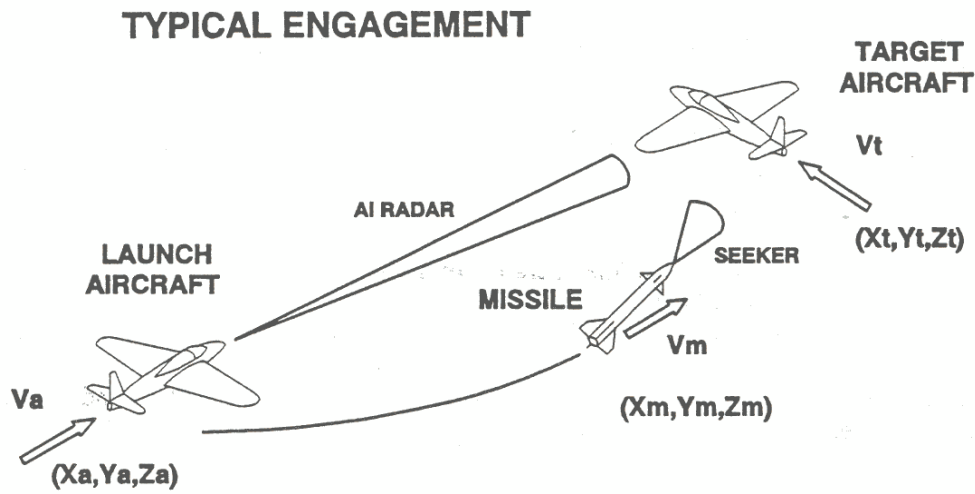
Figure 3-1: Typical Simulation Engagement

5 DoF Launch Aircraft

The launch aircraft is modeled as a modified point-mass with angle-of-attack and simplified pitch and roll dynamics (also referred to as 'pseudo 5-DOF'). For this research, the launch aircraft was constrained to be non-maneuvering with constant velocity (maintained straight and level flight path). No modifications were made to this model for the research described in this paper.

3 DoF Target Aircraft

The target aircraft is modeled as a simplified point-mass. The target maintained a straight and level flight path while holding constant velocity. This setup for the target

aircraft was sufficient for the scope of this research. No modifications were made to this model.

6 DoF Missile

The 6 degree-of-freedom missile model provided by ADNW previously had not been implemented into a simulation that was suitable for this research. The 6-DOF missile model replace a point-mass missile model in the existing 1 vs. 0 simulation provided by ADNW. The original DIME Two Axis Gimbal model and the DIME Simple Seeker model that were implemented into the original simulation were too complex for the scope of this research. (DIME stands for the Air Force Research Laboratories Munitions Directorate Dense Inert Metal Explosives Laboratory). These models were replaced with a much less complex Momentum Gimbal model and a Perfect Seeker model, respectfully.

TELEMON TRAP Perfect Seeker and TRAP Momentum Gimbal

The DIME Simple seeker and the DIME two-axis gimbal included in the original simulation were overly complicated for the purpose of this research. These models were replaced with the simple TRAP Perfect Seeker and TRAP Momentum Gimbal. For the perfect seeker, the seeker axis is always constrained to point at the target (subject to gimbal biases and limits) and the seeker line-of-sight rate commands are set to the true line-of-sight rate resolved into vertical and horizontal commands in the body axis (the body xz-plane and xy-plane). The seeker line-of-sight rate commands are limited to the input maximum line-of-sight tracking rate. The momentum gimbal is modeled for the

momentum-stabilized seeker platform. The seeker x-axis is initially constrained to point

at the target and gimbal angles are calculated according to the orientation of the gimbal

cages. Gimbal biases are input in pitch and yaw, and then are added to the gimbal angles.

The gimbal angles in either pitch or yaw are then limited to the input maximum gimbal

angle. The resulting gimbal angles are used to calculate a new seeker-reference-axes to

seeker-axes transformation matrix and hence a new reference-axes to seeker-axes

transformation matrix. This matrix is used to determine the geometric line-of-sight

angular tracking errors in the seeker. For the perfect seeker, these tracking errors are

always zero when the gimbal angles are not limited and providing the gimbal angle

biases are zero.

3.3 Missile Aerodynamic Model

Now that the overall architecture of the 1 vs. 0 Missile engagement simulation has

been introduced, more detail is going to be presented on the 6-DoF missile model used in

the simulation.

The aerodynamic methodology applied to the generic missile model used in this

research is based upon the aerodynamic methodology from the NASIC/ADNA software

called, the Trajectory Analysis Program, or TRAP for short. TRAP has been widely used

to evaluate the performance of aerodynamic vehicles in 1-vs-0 engagement scenarios.

Sections 3.3.1, 3.3.2 and 3.3.3 come from Reference 6.

3.3.1 Aerodynamic Angle Definitions

Aerodynamic characteristics are treated as a function of total angle-of-attack $\left(\alpha^{'}\right)$ and aerodynamic roll angle $\left(\phi^{'}\right)$. The relationship between these angles and the missile velocity components along the missile body x-axis (MVELBX = u), y-axis (MVELBY = v) and z-axis (MVELBZ = w) are shown in Figure 3-2. The equations relating the angles to the missile velocity components are:

$$\alpha^{'} = \tan^{-1}\left(\frac{\sqrt{v^2 + w^2}}{u}\right) \tag{3.1}$$

$$\phi^{'} = \tan^{-1}\frac{v}{w} \tag{3.2}$$

Figure 3-2 also shows two additional angles, these are PHIPRM and OFFPHI. PHIPRM is the aerodynamic roll angle for the aerodynamic characteristics and is always measured from the plane containing control surfaces 1 and 3, with control surface 1 to leeward for PHIPRM = 0.0. The angle OFFPHI is the offset angle between the zero body roll angle of the body (in this case, the top of the body is mid-way between controls 1 and 4) and zero aerodynamic roll angle for the aerodynamic characteristics. OFFPHI is positive if the missile must be rolled in the positive direction (clockwise looking along the missile body x-axis) when moving from zero aerodynamic roll angle (PHIPRM = 0.0) to zero body roll angle (PHIMSL = 0.0). Figure 3-2 shows the relationship between PHIPRM and OFFPHI for both a '+' and an 'X" configuration missile (OFFPHI = 0.0 and 45.0 degrees, respectively).
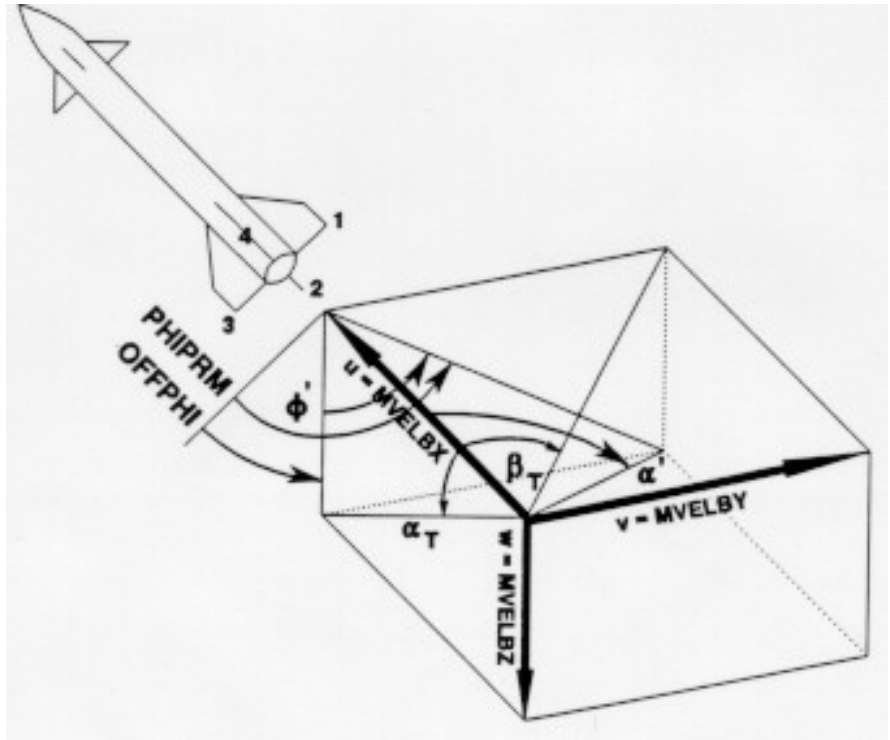
Figure 3-2: Aerodynamic Angles

3.3.2 Control Surface Deflection Conventions

The aerodynamic methodology uses the concept of effective pitch and yaw control deflections along with the net roll control deflection and the net squeeze control deflection. These each involve different combinations of individual control surface deflections. The conventions used by the aerodynamic methodology for defining control surface deflections are described in the sections below for individual control surface deflections, effective pitch control deflection, effective yaw control deflection and roll control deflection.

Individual Control Surface Deflections

The convention used for the individual control surface deflections denotes a positive control deflection as a clockwise rotation of the fin, from looking outboard from the missile, see Figure 3-3.
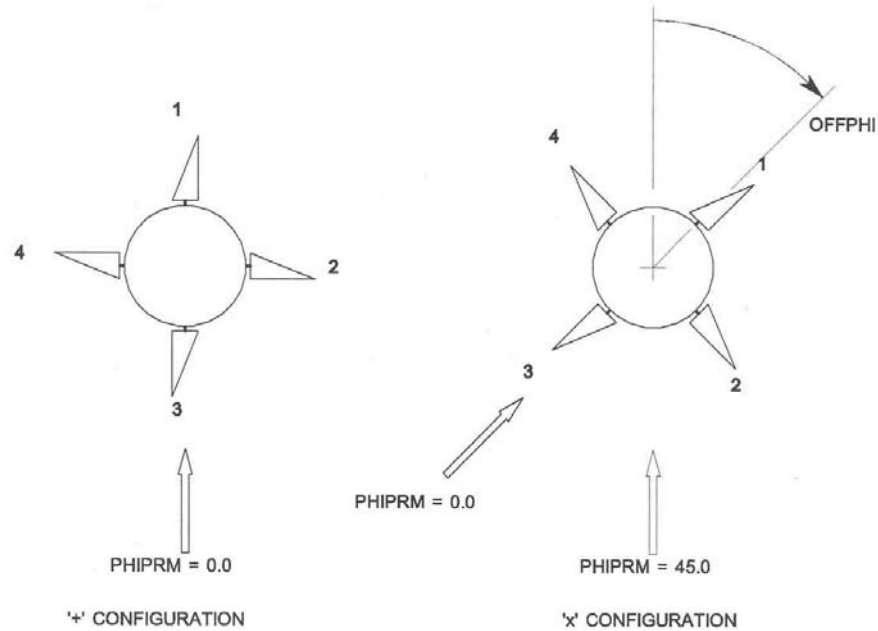
Figure 3-3: Individual Control Deflection Convention

Effective Pitch Control Deflection

The effective pitch control deflection is the sum of the individual control surface deflections resolved into the total angle-of-attach plane according to the equation:

$$\delta Q = 0.5(\delta 2 - \delta 4)\cos(PHIPRM) + 0.5(\delta 1 - \delta 3)\sin(PHIPRM) \qquad (3.3)$$

where DELQA = δQ is the effective pitch control deflection.

Figure 3-4: Effective Pitch Control Deflection

Figure 3-4 shows the maximum values of DELQA when the missile is at three different

aerodynamic roll angles (PHIPRM = 0.0, 26.57, 45.0 degrees). For the example shown

in the figure, the maximum deflection of an individual control is 20.0 degrees. This in

turn gives the maximum values of DELQA of 20.0, 22.36 and 28.28 degrees at the three

values of PHIPRM, respectively. The maximum values follow the relationship:

$$\max(DELQA) = \frac{\max(\delta)}{\cos(PHIPRM)} \qquad (3.4)$$

where $\max(\delta)$ is the maximum value for an individual control surface deflection. For the

purposes of the aerodynamic tables, it is inconvenient to have different maximum values

of one of the independent variables (DELQA) associated with each value of another of

the independent variables (PHIPRM). To alleviate this, the values of DELQA are

normalized by multiplying the actual value of DELQA by the cosine of PHIPRM.   The

illustration in Figure 3-4 shows examples of individual control deflections that produce only an effective pitch control deflection. As a result, the magnitude of the normalized value will never exceed the maximum magnitude of an individual control surface deflection. It is possible, however, to obtain normalized values of the effective pitch control deflection that are greater in magnitude than the maximum magnitude of an individual control surface deflection and exceed the maximum value in the data table. This occurs when the demand plane is not aligned with the total angle-of-attack plane. In such cases, the effective pitch control data will be extrapolated to the required value of effective pitch control deflection.

Effective Yaw Control Deflection

The effective yaw control surface deflection is the sum of the individual control surface deflections resolved normal to the total angle-of-attack plane according to the equation:

$$\delta R = 0.5(\delta 3 - \delta 1)\cos(PHIPRM) + 0.5(\delta 2 - \delta 4)\sin(PHIPRM) \qquad (3.5)$$

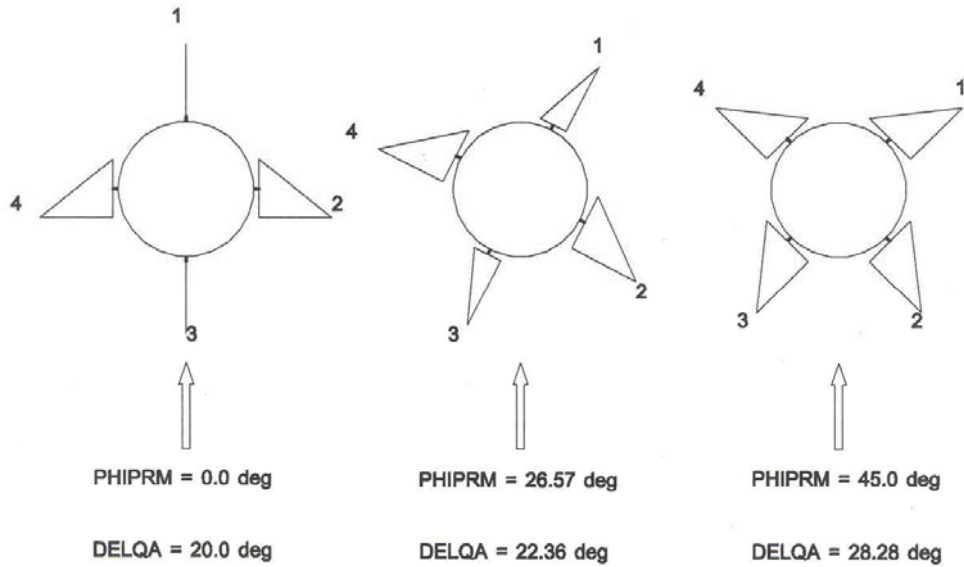Where DELRA = δR is the effective yaw control deflection. Figure 3-5 shows the maximum values of DELRA when the missile is at three aerodynamic roll angles (PHIPRM = 0.0, 26.57 and 45.0 degrees). In the figure, the maximum deflection is assumed to be 20.0 degrees which gives rise to the maximum values of DELRA of 20.0, 22.36 and 28.28 at the three values of PHIPRM, respectively.

The effective yaw control deflection is never used as an independent variable in the data tables. The treatment of the effective yaw control deflection is handled through the use of aerodynamic derivatives, which are assumed to be independent of the magnitude of the

effective yaw control deflection. As a result, there is no need to normalize the values of the effective yaw control surface deflection. This use of aerodynamic derivatives can be rationalized because the magnitude of the effective yaw control deflection will generally be small. Large effective yaw control deflections usually occur in transient situations and are of short duration.
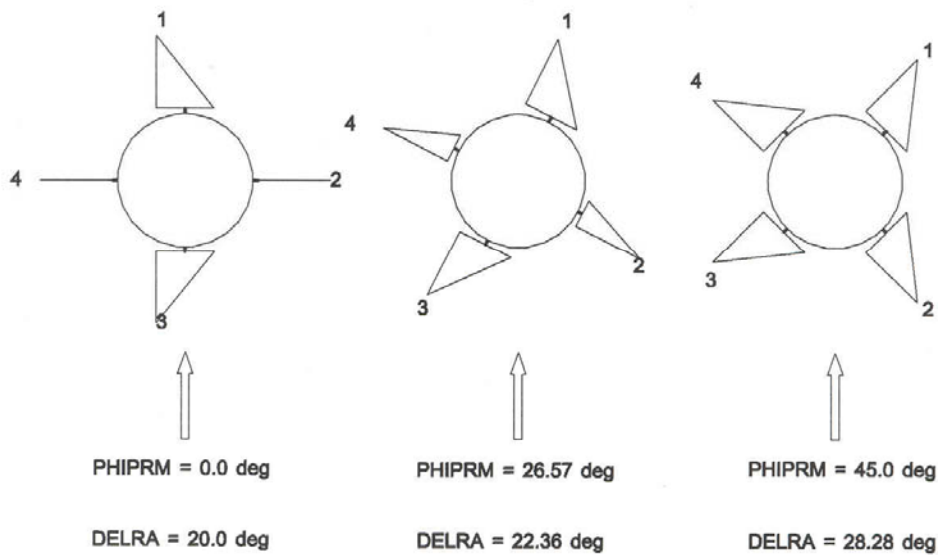
Figure 3-5: Effective Yaw Control Deflection

Roll Control Deflection

The net roll control deflection is defined by the equation:

$$\delta P = 0.25(\delta 1 + \delta 2 + \delta 3 + \delta 4) \tag{3.6}$$

Where DELPA = δP is the net roll control deflection. A pure roll command is shown in Figure 3-6 where all the control surfaces are deflected by equal amounts in the same direction by 10.0 degrees.
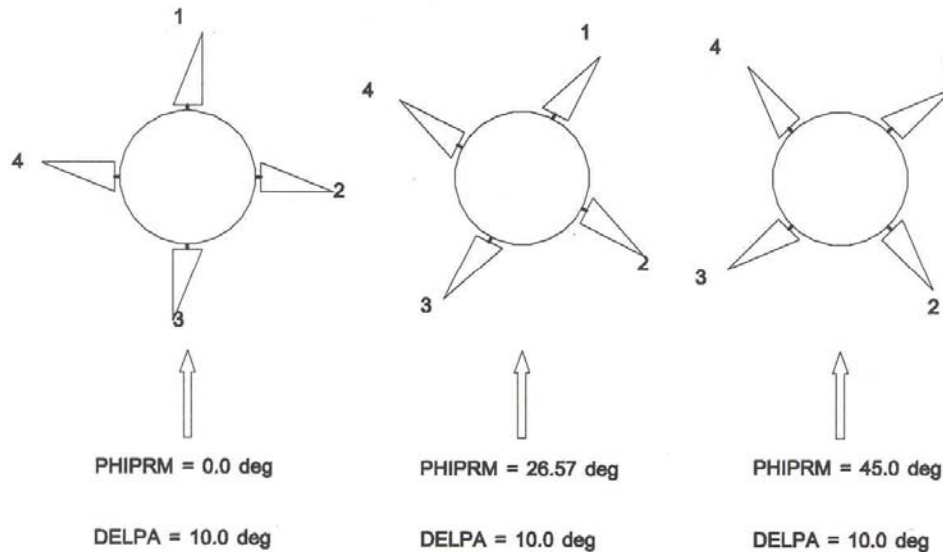
Figure 3-6: Roll Control Deflection

The net roll control deflection is never used as an in dependent variable in the data tables.
The treatment of the net roll control deflection is handled through the use of aerodynamic
derivatives, which are assumed to be independent of the magnitude of the net roll control
deflection. This approach is rationalized because of the relatively small magnitudes that
are usually associated with the net roll control deflections.

Squeeze Control Deflection

There is a combination of individual control surface deflections that produce no net
moment and no lateral force, only an increase in the axial force. This is called the
squeeze control deflection. The net squeeze control deflection is defined by the equation:

$$\delta S = 0.25(\delta 1 - \delta 2 + \delta 3 - \delta 4) \qquad (3.7)$$

Where DELSA $= \delta S$ is the net squeeze control deflection. A pure squeeze control is illustrated in Figure 3-7, where the maximum deflection for each individual control surface shown is 10.0 degrees. It is of interest for control system design to keep the net squeeze control deflection to zero, since the main function of the squeeze control is to contribute to the axial force.

PHIPRM = 0.0 deg   PHIPRM = 26.57 deg   PHIPRM = 45.0 deg

DELSA = 10.0 deg   DELSA = 10.0 deg   DELSA = 10.0 deg
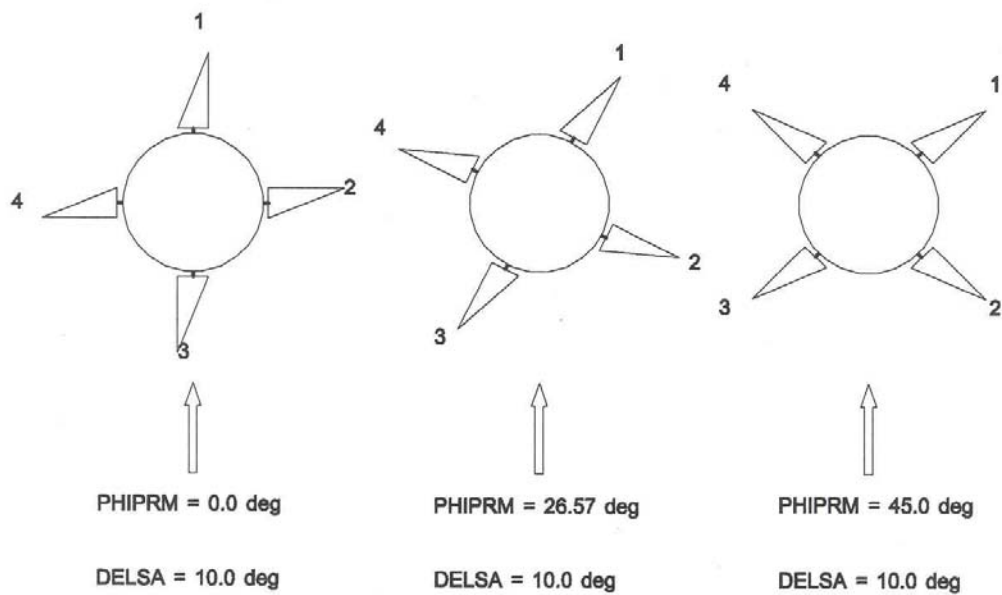
Figure 3-7: Squeeze Control Deflection

Combinations of Control Surface Deflections

The relationship between the individual control surface deflections $(\delta 1, \delta 2, \delta 3, \delta 4)$ and the various definitions of combined control surface deflections $(\delta P, \delta Q, \delta R, \delta S)$ can be represented by collecting the equations above and expressing them in the matrix form:

$$\begin{bmatrix} \delta P \\ \delta Q \\ \delta R \\ \delta S \end{bmatrix} = \frac{1}{4} \begin{bmatrix} 1 & 1 & 1 & 1 \\ 2\sin\phi & 2\cos\phi & -2\sin\phi & -2\cos\phi \\ -2\cos\phi & 2\sin\phi & 2\cos\phi & -2\sin\phi \\ 1 & -1 & 1 & -1 \end{bmatrix} \begin{bmatrix} \delta 1 \\ \delta 2 \\ \delta 3 \\ \delta 4 \end{bmatrix} \quad (3.8)$$

Where ϕ is defined as PHIPRM, the aerodynamic roll angle. By inverting the above

matrix, the individual control surface deflections $(\delta 1, \delta 2, \delta 3, \delta 4)$ can be determined given

any set of combined control deflections $(\delta P, \delta Q, \delta R, \delta S)$.

$$\begin{bmatrix} \delta 1 \\ \delta 2 \\ \delta 3 \\ \delta 4 \end{bmatrix} = \begin{bmatrix} 1 & \sin\phi & -\cos\phi & 1 \\ 1 & \cos\phi & \sin\phi & -1 \\ 1 & -\sin\phi & \cos\phi & 1 \\ 1 & -\cos\phi & -\sin\phi & -1 \end{bmatrix} \begin{bmatrix} \delta P \\ \delta Q \\ \delta R \\ \delta S \end{bmatrix} \quad (3.9)$$

By applying the constraint of zero squeeze control deflection to the above equation, the

relationship between the individual control deflections and three axes control deflections

is determined:

$$\begin{bmatrix} \delta 1 \\ \delta 2 \\ \delta 3 \\ \delta 4 \end{bmatrix} = \begin{bmatrix} 1 & \sin\phi & -\cos\phi \\ 1 & \cos\phi & \sin\phi \\ 1 & -\sin\phi & \cos\phi \\ 1 & -\cos\phi & -\sin\phi \end{bmatrix} \begin{bmatrix} \delta P \\ \delta Q \\ \delta R \end{bmatrix} \quad (3.10)$$

3.3.3 Aerodynamic Coefficients

This section describes the aerodynamic coefficients that are included in the

modeling of the 6-DOF missile used in this research. The coefficients described in this

section will be incorporated into the forces and moments equations in the next sections of

this report.

Basic Airframe Aerodynamics

There are six aerodynamic coefficients that describe the characteristics of the basic airframe without any control deflection. These are:

CA	Axial force coefficient
$CN_{\alpha'}$	Normal force coefficient, measured in the total angle-of -attack plane
$CMREF_{\alpha'}$	Pitch moment coefficient about the reference center-of-gravity location, measured in the total angle-of-attack plane.
$CY_{\alpha'}$	Side force coefficient, measured normal to the total angle-of-attack plane.
$CLNREF_{\alpha'}$	Yaw moment coefficient about the reference center-of-gravity location, measured normal to the total angle-of-attack plane.
CLL	Roll moment coefficient

Five of these coefficients are a function of the aerodynamic roll angle, total angle-of-attack and Mach number. Note that the subscript α' denotes that the coefficient is referenced to the total angle-of-attack plane.

Airframe Aerodynamics with Control Effects

There are six aerodynamic coefficients and 12 static aerodynamic derivatives that describe the incremental aerodynamic characteristics due to control deflection. The six aerodynamic coefficients are associated with the effective pitch control deflection. Six of the 12 aerodynamic derivatives are associated with the roll control deflection and six are associated with the effective yaw control deflection.

Effective Pitch Control Deflection

Because the missile maneuvers primarily in the total angle-of-attack plane, the effective pitch control deflection (δQ) is likely to be any value up to the maximum physical limits of the controls. Therefore, the effect of the effective pitch control deflections is treated by considering the actual deflection rather than using an aerodynamic derivative. The impact of effective pitch control deflection on each of the six basic aerodynamic coefficients is given by:

$\Delta(CA)_{\delta Q}$ Incremental axial force coefficient due to effective pitch control deflection, δQ.

$\Delta(CN_{\alpha'})_{\delta Q}$ Incremental normal force coefficient due to effective pitch control deflection, δQ.

$\Delta(CMREF_{\alpha'})_{\delta Q}$ Incremental pitch moment coefficient about the reference center-of-gravity location due to effective pitch control deflection, δQ.

$\Delta(CY_{\alpha'})_{\delta Q}$ Incremental side force coefficient due to effective pitch control deflection δQ, measured normal to the total angle-of-attack plane.

$\Delta(CLNREF_{\alpha'})_{\delta Q}$ Incremental yaw moment coefficient about the reference center-of-gravity location due to effective pitch control deflection δQ, measured normal to the total angle-of-attack plane.

$\Delta(CLL)_{\delta Q}$ Incremental roll moment coefficient due to effective pitch control deflection, δQ.

The use of the prefix Δ indicates that this is an incremental value in the coefficient and the suffix δQ indicates that it is due to a specific value of effective pitch control deflection, δQ. Note that, by definition, the total angle-of-attack can only be positive

which means, for a statically stable missile that is tail controlled, a trim condition must always be associated with a negative value of δQ. These coefficients are a function of the effective pitch control deflection, total angle-of-attack, aerodynamic roll angle and Mach number.

Roll Control Deflection

Because missiles generally have small roll moments-of-inertia compared to the aerodynamic roll moment that can be developed by the control surfaces, usually only small control surface deflections are required in roll. It is desired then to use aerodynamic derivatives that are independent of the magnitude of the roll control deflections to define the roll control effects. The effect of roll control deflection (δP) on the aerodynamic coefficients is given by:

$\left(\dfrac{dCA}{dP^2} \right)_{\delta Q}$ Rate of change of the axial force coefficient with the square of the roll control deflection, δP.

$\left(\dfrac{dCN_{\dot{\alpha}}}{dP^2} \right)_{\delta Q}$ Rate of change of the normal force coefficient with the square of the roll control deflection δP, measured in the total angle-of-attack plane.

$\left(\dfrac{dCMREF_{\dot{\alpha}}}{dP^2} \right)_{\delta Q}$ Rate of change of the pitch moment coefficient about the reference center-of-gravity with the square of the roll control deflection δP, measured in the total angle-of-attack plane.

$\left(\dfrac{dCY_{\dot{\alpha}}}{dP} \right)_{\delta Q}$ Rate of change of the side force coefficient with the roll control deflection δP, measured normal to the total angle-of-attack.

$\left(\dfrac{dCLNREF_{\alpha}}{dP} \right)_{\delta Q}$ Rate of change of the yaw moment coefficient about the reference

center-of-gravity with the roll control deflection δP, measured normal

to the total angle-of-attack plane.

$\left(\dfrac{dCLL}{dP} \right)_{\delta Q}$ Rate of change of the roll moment coefficient with the roll control

deflection δP.

The use of the suffix, δQ indicates that the aerodynamic derivative applies at a specific

value of effective pitch control deflection δQ. The above aerodynamic derivatives are a

function of the effective pitch control deflection, total angle-of-attack, aerodynamic roll

angle and Mach number.

Effective Yaw Control Deflection

When the maneuver demand plane and total angle-of-attack plane are not aligned,

the result of resolving the individual control deflections normal to the total angle-of-

attack plane is termed the effective yaw control deflection. However, because the

demand plane and total angle-of-attack plane are generally close to being aligned, the

magnitude of the effective yaw control deflection is usually very small. It is desired then

to use aerodynamic derivatives that are independent of the magnitude of the effective

yaw control deflections to define the effective yaw control effects. The effect of the

effective yaw control deflection (δR) on the aerodynamic coefficients is given by:

$\left(\dfrac{dCA}{dR^2} \right)_{\delta Q}$ Rate of change of the axial force coefficient with the square of the

effective yaw control deflection δR.

$$\left(\frac{dCN_{\alpha^{'}}}{dR^2}\right)_{\delta Q}$$

Rate of change of the normal force coefficient with the square of the effective yaw control deflection δR, measured in the total angle-of-attack plane.

$$\left(\frac{dCMREF_{\alpha^{'}}}{dR^2}\right)_{\delta Q}$$

Rate of change of the pitch moment coefficient about the reference center-of-gravity with the square of the effective control deflection δR, measured in the total angle-of-attack plane.

$$\left(\frac{dCY_{\alpha^{'}}}{dR}\right)_{\delta Q}$$

Rate of change of the side force coefficient with the effective control deflection δR, measured normal to the total angle-of-attack Plane.

$$\left(\frac{dCLNREF_{\alpha^{'}}}{dR}\right)_{\delta Q}$$

Rate of change of the yaw moment coefficient about the reference center-of-gravity with the effective yaw control deflection δR, measured normal to the total angle-of-attack plane.

$$\left(\frac{dCLNREF_{\alpha^{'}}}{dR}\right)_{\delta Q}$$

Rate of change of the roll moment coefficient with the effective yaw control deflection, δR.

The use of the suffix δQ indicates that the aerodynamic derivative applies at a specific value of effective pitch control deflection, δQ. The above aerodynamic derivatives are a function of the effective pitch control deflection, total angle-of-attack, aerodynamic roll angle and Mach number.

The coefficients described in this section will be incorporated into the forces and moments equations in the next section of this report.

3.3.4 Aerodynamic Forces and Moments Coefficient Equations

This section describes the steps taken in the missile aerodynamic model to determine the aerodynamic forces and moments equations used to derive the translational and rotational equations of motion of the missile airframe.

First, the α' - ϕ' partial aerodynamic coefficients are combined into the six primary force and moment coefficient equations in the wind axis system. The total aerodynamic force coefficient terms, including both longitudinal and lateral coefficients are:

$$CA_{tot} = CA_0 + \Delta(CA)_{\delta Q} + \left(\frac{dCA}{dP^2}\right)_{\delta Q} (\delta P)^2 + \left(\frac{dCA}{dR^2}\right)_{\delta Q} (\delta R)^2 \qquad (3.11)$$

$$CY_{\alpha' tot} = CY_{\alpha' 0} + \Delta(CY_{\alpha'})_{\delta Q} + \left(\frac{dCY_{\alpha'}}{dP}\right)_{\delta Q} \delta P + \left(\frac{dCY_{\alpha'}}{dR}\right)_{\delta Q} \delta R \qquad (3.12)$$

$$CN_{\alpha' tot} = CN_{\alpha' 0} + \Delta(CN_{\alpha'})_{\delta Q} + \left(\frac{dCN_{\alpha'}}{dP^2}\right)_{\delta Q} (\delta P)^2 + \left(\frac{dCN_{\alpha'}}{dR^2}\right)_{\delta Q} (\delta R)^2 \qquad (3.13)$$

The total aerodynamic moment coefficient terms, including both longitudinal and lateral coefficients are:

$$CLL_{tot} = CLL_0 + \Delta(CLL)_{\delta Q} + \left(\frac{dCLL}{dP}\right)_{\delta Q} \delta P + \left(\frac{dCLL}{dR}\right)_{\delta Q} \delta R \qquad (3.14)$$

$$CMREF_{\alpha' tot} = CMREF_{\alpha' 0} + \Delta(CMREF_{\alpha'})_{\delta Q} + \left(\frac{dCMREF_{\alpha'}}{dP^2}\right)_{\delta Q} (\delta P)^2 + \left(\frac{dCMREF_{\alpha'}}{dR^2}\right)_{\delta Q} (\delta R)^2 \quad (3.15)$$

$$CLNREF_{\alpha_{tot}} = CLNREF_{\alpha_0} + \Delta(CLNREF_\alpha)_{\delta Q} + \left(\frac{dCLNREF_\alpha}{dP}\right)_{\delta Q} \delta P + \left(\frac{dCLNREF_\alpha}{dR}\right)_{\delta Q} \delta R \quad (3.16)$$

Where the suffix '0' indicates the un-deflected "basic stability" coefficient.

Next, the six primary missile aerodynamic coefficients described in Equations 3.11 - 3.16 are transformed from the α' - ϕ' Aeroballistic coordinate system into the Body Axis coordinate system with the use of the coordinate transformation matrix:

$$[T] = \begin{bmatrix} \cos\alpha' & \sin\alpha' \sin\phi' & \sin\alpha' \cos\phi' \\ 0 & \cos\phi' & -\sin\phi' \\ -\sin\alpha' & \cos\alpha' \sin\phi' & \cos\alpha' \cos\phi' \end{bmatrix} \quad (3.17)$$

Before the forces and moment equations can be developed, the dynamic damping terms need to be added to the three moment coefficients in Equations 3.14 – 3.16. These terms consist of damping derivative, control effectiveness and center of gravity, c.g. adjustments. Rewriting Equations 3.14-3.16 with these terms gives:

$$CLL_{tot} = CLL_0 + \Delta(CLL)_{\delta Q} + C_{l_P} \frac{pl}{2V} + \left(\frac{dCLL}{dP}\right)_{\delta Q} \delta P + \left(\frac{dCLL}{dR}\right)_{\delta Q} \delta R \quad (3.18)$$

$$CMREF_{\alpha'_{tot}} = CMREF_{\alpha'_0} + \Delta(CMREF_{\alpha'})_{\delta Q} + C_{m_q} \frac{ql}{2V} + \frac{CN_{\alpha'}(x_{cg,ref} - x_{cg})}{l} + ...$$

$$(3.19)$$

$$\left(\frac{dCMREF_{\alpha'}}{dP^2}\right)_{\delta Q} (\delta P)^2 + \left(\frac{dCMREF_{\alpha'}}{dR^2}\right)_{\delta Q} (\delta R)^2$$

$$CLNREF_{\alpha\,tot} = CLNREF_{\alpha\,0} + \Delta(CLNREF_{\alpha})_{\delta Q} + C_{n_r}\frac{rl}{2V} + \frac{CY_{\alpha}(x_{cg,ref} - x_{cg})}{l} + ...$$

$$(3.20)$$

$$\left(\frac{dCLNREF_{\alpha}}{dP}\right)_{\delta Q}\delta P + \left(\frac{dCLNREF_{\alpha}}{dR}\right)_{\delta Q}\delta R$$

Where,

C_{l_P} Variation of rolling moment coefficient with rate of change of roll rate

C_{m_q} Variation of pitching moment coefficient with pitch rate

C_{n_r} Variation of yawing moment coefficient with rate of change of yaw rate

p Roll rate of the missile

q Pitch rate of the missile

r Yaw rate of the missile

l Missile aerodynamic reference length

V Airspeed

$x_{cg,ref}$ Reference Center-of-gravity of nose where the Aerodynamic tables were

generated from.

x_{cg} Center-of-gravity of missile

3.3.5 Accounting for First Order Effects

Before continuing on to the forces and moments equations, the forces and

moment coefficient terms must be simplified to include only first order effects. The

aerodynamic data used in the missile model does not include second-order effects

because, Missile DATCOM, the semi-empirical prediction software used to create the aerodynamic data is not capable of generating any second-order control effects.

The first-order aerodynamic characteristics are classed as those in which the control surface deflection has a primary effect on the particular aerodynamic coefficient. The first-order effects are the effect of any of the three control deflections (δQ, δP, δR) on the axial force coefficient, the effect of δQ on the normal force and pitch moment coefficients, the effect of δP on the roll moment coefficient and the effect of δR on the side force and yaw moment coefficients.[6]

The first-order terms are as follows:

Basic stability coefficients:

$$CA, CN_{\alpha'}, CMREF_{\alpha'}, CY_{\alpha'}, CLNREF_{\alpha'}, CLL$$

Incremental coefficients:

$$\Delta(CA)_{\delta Q}, \Delta(CN_{\alpha'})_{\delta Q}, \Delta(CMREF_{\alpha'})_{\delta Q}$$

Aerodynamic derivatives:

$$\left(\frac{dCA}{dP^2}\right)_{\delta Q}, \left(\frac{dCLL}{dP}\right)_{\delta Q}, \left(\frac{dCA}{dR^2}\right)_{\delta Q}, \left(\frac{dCY_{\alpha'}}{dR}\right)_{\delta Q}, \left(\frac{dCLNREF_{\alpha'}}{dR}\right)_{\delta Q}$$

Equations 3.11-3.13 and 3.18-3.20 are re-written to include only the first-order terms:

For the total force coefficient terms:

$$CA_{tot} = CA_0 + \Delta(CA)_{\delta Q} + \left(\frac{dCA}{dP^2}\right)_{\delta Q}(\delta P)^2 + \left(\frac{dCA}{dR^2}\right)_{\delta Q}(\delta R)^2 \tag{3.21}$$

$$CY_{\alpha' tot} = CY_{\alpha' 0} + \left(\frac{dCY_{\alpha'}}{dR}\right)_{\delta Q} \delta R \tag{3.22}$$

$$CN_{\alpha'_{tot}} = CN_{\alpha'_0} + \Delta(CN_{\alpha'})_{\delta Q} \tag{3.23}$$

For the total moment coefficient terms:

$$CLL_{tot} = CLL_0 + C_{l_P} \frac{pl}{2V} + \left(\frac{dCLL}{dP}\right)_{\delta Q} \delta P$$

(3.24)

$$CMREF_{\alpha'_{tot}} = CMREF_{\alpha'_0} + \Delta(CMREF_{\alpha'})_{\delta Q} + C_{m_q} \frac{ql}{2V} + \frac{CN_{\alpha'}\left(x_{cg,ref} - x_{cg}\right)}{l} \tag{3.25}$$

$$CLNREF_{\alpha'_{tot}} = CLNREF_{\alpha'_0} + C_{n_r} \frac{rl}{2V} + \frac{CY_{\alpha'}\left(x_{cg,ref} - x_{cg}\right)}{l} + \left(\frac{dCLNREF_{\alpha'}}{dR}\right)_{\delta Q} \delta R \tag{3.26}$$

3.3.6 Equations of Motion

The equations of motion presented here are for a missile over a flat Earth. Now that the force and moment coefficients have been defined with first-order terms, the forces and moments equations now can be presented.

The force equations are:

$$F_1 = -qSCA_{tot} + THRUST \tag{3.27}$$

$$F_2 = qSCY_{\alpha'_{tot}}$$

(3.28)

$$F_3 = -qSCN_{\alpha'_{tot}}$$

(3.29)

The moment equations are:

$$M_1 = qSdCLL \tag{3.30}$$

$$M_2 = qSdCMREF_{\dot{\alpha}\,tot} \tag{3.31}$$

$$M_3 = qSdCLNREF_{\dot{\alpha}\,tot} \tag{3.32}$$

Where,

q Dynamic pressure

S Reference Area

d Missile Diameter

Now the traslational and rotational equation of motion for the missile model can be presented. The translational degrees of freedom, represented by the velocity components u, v and w, are solved by Newton's equation; and the rotational DoF, which are expressed in body rates p, q and r, are governed by Euler's equation.[7] Newton's second law with respect to Earth, as the inertial reference frame, states that the time rate of change of linear momentum equals the externally applied forces. Newton's Equations for the translational DoF are:

$$\frac{du}{dt} = rv - qw + \frac{F_1}{m} + t_{13}\,g \tag{3.33}$$

$$\frac{dv}{dt} = pw - ru + \frac{F_2}{m} + t_{23}\,g \tag{3.34}$$

$$\frac{du}{dt} = qu - pv + \frac{F_3}{m} + t_{33}\,g \tag{3.35}$$

Where,

t Element in the direction cosine matrix

g Acceleration due to gravity

Euler's law states that the time rate of change of angular momentum equals the externally

applied moments.[7] Euler's Equations for the rotational DoF are:

$$\frac{dp}{dt} = I_{xx}^{-1}\left(\left(I_{yy} - I_{zz}\right)qr + m_1\right) \tag{3.36}$$

$$\frac{dq}{dt} = I_{yy}^{-1}\left(\left(I_{zz} - I_{xx}\right)pr + m_2\right) \tag{3.37}$$

$$\frac{dr}{dt} = I_{zz}^{-1}\left(\left(I_{xx} - I_{yy}\right)pq + m_3\right) \tag{3.38}$$

3.3.7 Aerodynamic Data Generation

The aerodynamic data for the 6-DoF missile model was based on a supersonic,

tail controlled missile with similar geometry and mass properties of an AIM-9X missile.

The data was generated using the semi-empirical prediction code, Missile DATCOM, or

MISDATA.

This section discusses the use of the aerodynamic prediction method, Missile

DATCOM, or MISDAT, to generate the aerodynamic table data required for the 6

degree-of-freedom SIMULINK missile model as presented by Reference 6. The fidelity

associated with semi-empirical prediction methods is such that in most instances, the

aerodynamic characteristics will repeat at every 90.0 degrees in aerodynamic roll angle.

This considerably reduced the amount of data that was required to represent the airframe

aerodynamic characteristics.

Basic Airframe Aerodynamics

The basic airframe aerodynamics consists of data on the missile configuration without the controls being deflected. Since the missile is modeled in the cruciform shape (PHIPRM = 0.0) and:

- Is assumed to have a small degree of asymmetry

- Does not operate at a high angle-of-attack,

The aerodynamic characteristics are well enough behaved to be repeated every 90.0 degrees in aerodynamic roll angle. Since this was the case, the data was obtained through a range of 45.0 degrees in aerodynamic roll angle, which captured a complete half cycle of the data. The number of intermediate roll angles depends on the behavior of the aerodynamic characteristics. The use of a small number of intermediate values can be accepted where the data are well behaved when combined with the use of Hermitian interpolation. The smallest increment used in the data set was + 5.0 degrees. A complete listing of all the basic airframe aerodynamic variables and the associated value ranges they were collected at is listed in Table 1.

Effect of Controls

For basic missile configurations that only exhibit a small degree of asymmetry, the incremental effect of the control deflections is very small. Therefore, for a cruciform missile with little asymmetries, the control effectiveness is provided over a 45.0 degree range of aerodynamic roll angle.

Since it is unlikely that semi-empirical prediction methods are capable of generating any of the second-order effects of the controls, the data set used in this research was limited

51

to first-order effects only. The first order effects are those in which the change in the aerodynamic coefficient is in the same plane in which the control deflection occurs. The first-order effects due to effective pitch control deflection are actual increments in the values of the aerodynamic coefficients. For the roll control deflection and effective yaw control deflection, the first order effects are represented by aerodynamic derivatives. A complete listing of all the effects of control variables and the associated value ranges they were collected at is listed in Table 1.

Table 3-1: Aerodynamic and Control Derivatives

Variable	Description	Function of:	Mach	Phi' (deg)	Alpha' (deg)	DelQ	Xcg
ACA0	Undeflected Axial Force	ϕ', α', M	0.4 to 5.0	0 to 45	0 to 25	N/A	N/A
ACN0	Undeflected Normal Force						
ACY0	Undeflected Side Force						
ACMRF0	Undeflected Pitching Moment						
ACNRF0	Undeflected Yaw Moment						
ACLL0	Undeflected Roll Moment						

Variable	Description	Function of:	Mach	Phi' (deg)	Alpha' (deg)	DelQ	Xcg
ADLCAQ	Incremental Axial Force	$\delta_e, \phi', \alpha', M$	0.4 to 5.0	[0 26.5 45.0]	0 to 25	-20 to 20	N/A
ADLCAP	Axial Force Deriv. (wrt d_a^2)						
ADLCAR	Axial Force Deriv. (wrt d_r^2)						
ADLCNQ	Incremental Normal Force						
ADLCNP	Normal Force Deriv. (wrt d_a^2)						
ADLCNR	Normal Force Deriv. (wrt d_r^2)						
ADLCYQ	Incremental Side Force						
ADLCYP	Side Force Deriv. (wrt d_a)						
ADLCYR	Side Force Deriv. (wrt d_r)						
ADCMRQ	Incremental Pitching Moment						
ADCMRP	Pitch Moment Deriv. (wrt d_a^2)						
ADCMRR	Pitch Moment Deriv. (wrt d_r^2)						
ADCNRQ	Incremental Yaw Moment						
ADCNRP	Yaw Moment Deriv. (wrt d_a)						
ADCNRR	Yaw Moment Deriv. (wrt d_r)						
ADCLLQ	Incremental Roll Moment						
ADCLLP	Roll Moment Deriv. (wrt d_a)						
ADCLLR	Roll Moment Deriv. (wrt d_r)						

Variable	Description	Function of:	Mach	Phi' (deg)	Alpha' (deg)	DelQ	Xcg
CMQ	Pitch Damping (wrt pitch rate)	M, XCG	0.4 to 5.0	N/A	N/A	N/A	[1.52 1.58 1.65]
CMAD	Pitch Damping (wrt alphadot)	M, XCG	0.4 to 5.0	N/A	N/A	N/A	[1.52 1.58 1.65]
CLP	Roll Damping	M	0.4 to 5.0	N/A	N/A	N/A	N/A

3.4 Missile Autopilot

The original missile model did not have an acceleration autopilot implemented; in order to control the missile during simulation, pitch plane and yaw plane acceleration autopilots were added. The acceleration autopilots were taken from Zipfel, Reference 7. Figure 3-8, obtained from Reference 7, shows a general diagram of the acceleration autopilot used in the missile simulation. Because this is a missile simulation, the yaw plane is implemented in the same way.

The acceleration tracking loops for both autopilots were designed using modern pole placement techniques. For best performance, proportional and integral (PI) techniques were applied. Proportional control was used for quick response and integral control was used for zeroing the steady-state errors. To improve performance, an inner rate loop was added for stability augmentation. The three feedback gains in the autopilots were solved to satisfy the specified closed-loop response.
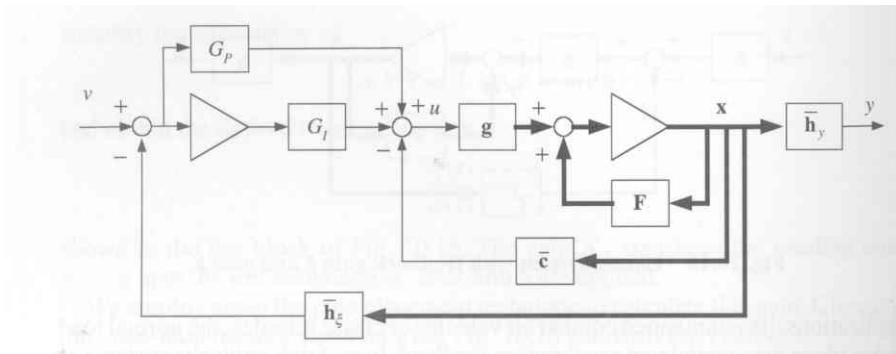

Figure 3-8: General Acceleration PI Autopilot

The linear time-variant plant is:

$$\dot{x} = F(t)x + g(t)u \tag{3.39}$$

From figure 3-8, the proportional and integral feed-forward branches with their

respective gains, G_P and G_I are easily visible. The major feedback loop is via the rate

and acceleration gains $\bar{c} = \begin{bmatrix} k_2 & k_1 \end{bmatrix}$. A second acceleration feedback with unit gain $\overline{h_\xi}$ is

wrapped around the outside to improve performance. The relationship for the control

variable can be derived from the figure.

$$u = -\bar{c}x + G_I \int (v - \overline{h_\xi}x)dt + G_P(v - \overline{h_\xi}x) \tag{3.40}$$

The states are then augmented by introducing the scalar auxiliary variable; in its state

equation form:

$$\dot{\xi} = v - \overline{h_\xi}x \tag{3.41}$$

Substituting u into the open-loop system yields the closed-loop system, augmented by the

auxiliary variable ξ:

$$\begin{bmatrix} \dot{x} \\ \dot{\xi} \end{bmatrix} = \begin{bmatrix} F - g(\bar{c} + G_P\overline{h_\xi}) & G_I g \\ -\overline{h_\xi} & 0 \end{bmatrix} \begin{bmatrix} x \\ \xi \end{bmatrix} + \begin{bmatrix} G_P g \\ 1 \end{bmatrix} v \tag{3.42}$$

Which can be abbreviated as:

$$\dot{x}' = F'(t)x' + g'(t)v \tag{3.43}$$

The eigenvalues of this closed-loop fundamental matrix F' must be equal to the desired

closed-loop poles. The condition for pole placement is:

$$\det \begin{Vmatrix} I_{nxn}s - F + g(\bar{c} + G_P\overline{h_\xi}) & -G_I g \\ \overline{h_\xi} & s \end{Vmatrix} = \prod_{i=1}^{n}(s - p_i) \tag{3.44}$$

Given the linearized longitudinal plant equation:

$$\begin{bmatrix} \dot{q} \\ \dot{a} \end{bmatrix} = \begin{bmatrix} M_q & \dfrac{M_\alpha}{N_\alpha} \\ N_\alpha & -\dfrac{N_\alpha}{V} \end{bmatrix} \begin{bmatrix} q \\ a \end{bmatrix} + \begin{bmatrix} M_\delta \\ 0 \end{bmatrix} \delta \tag{3.45}$$

where a is the normal acceleration, and:

$$N_\alpha = \frac{\overline{q}S}{m} C_{N_\alpha} \tag{3.46}$$

$$M_q = \frac{\overline{q}Sd^2}{2I_2 V} C_{m_q} \tag{3.47}$$

$$M_\alpha = \frac{\overline{q}Sd}{I_2} C_{m_\alpha} \tag{3.48}$$

$$M_{\delta q} = \frac{\overline{q}Sd}{I_2} C_{m_{\delta q}} \tag{3.49}$$

For the condition of pole placement, the corresponding equations are:

$$\overline{x} = \begin{bmatrix} q & a \end{bmatrix} \tag{3.50}$$

$$F = \begin{bmatrix} M_\alpha & \dfrac{M_\alpha}{N_\alpha} \\ N_\alpha & -\dfrac{N_\alpha}{V} \end{bmatrix} \tag{3.51}$$

$$\overline{g} = \begin{bmatrix} M_\delta & 0 \end{bmatrix} \tag{3.52}$$

$$u = \delta \tag{3.53}$$

$$\overline{h_\xi} = \begin{bmatrix} 0 & 1 \end{bmatrix} \tag{3.54}$$

$$\bar{c} = \begin{bmatrix} k_2 & k_1 \end{bmatrix} \tag{3.55}$$
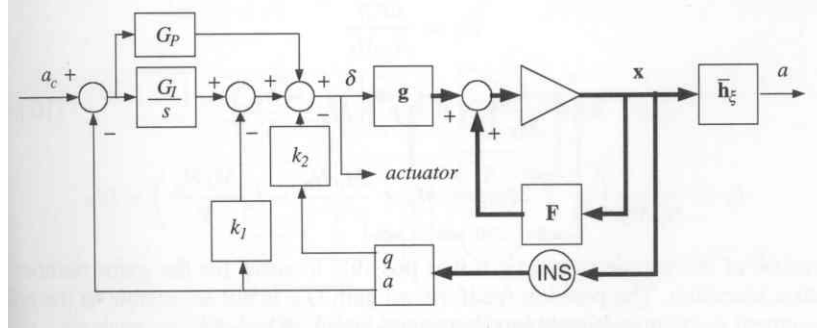

Figure 3-9 Acceleration Autopilot for Missile

Figure 3-9 shows in detail, the variables described above added to Figure 3-8 (from

Reference 7). This schematic was directly implemented into the model simulation

SIMULINK code. The gains k_1, k_2 and G_I are calculated from the pole placement

condition equation (3-11). Evaluating the left-hand determinant and equating terms of

equal power yields the three gains:

$$G_I = \frac{\omega^2 p}{N_\alpha M_\delta} \tag{3.56}$$

$$k_2 = \frac{1}{M_\delta} \left(2\zeta\omega + p + M_q - \frac{N_\alpha}{V} \right) \tag{3.57}$$

$$k_1 = \frac{1}{N_\alpha M_\delta} \left(\omega^2 + 2\zeta\omega p + M_\alpha + \frac{M_q N_\alpha}{V} - k_2 \frac{M_\delta N_\alpha}{V} \right) - G_P \tag{3.58}$$

The autopilot was implemented into the simulation to calculate these gains on-line with changing airframe conditions. The system dynamic characteristics, natural frequency, damping and pole location values chosen were evaluated over the missile flight envelope to ensure stability and desired system behavior. The solution for the position feed-forward gain G_P is not accessible by the pole placement technique and was determined based on root locus analysis of the system.

To summarize, this chapter laid the background needed to understand the Missile simulation created in SIMULINK that was used for this research. Chapter 4 will now utilize outputs generated from running the simulation along with the linear regression methods described in Chapter 2 to analyze linear regression as a tool for parameter ID of a missile.

4. Results and Analysis

4.1 Aerodynamics of the Experiment

This research focused on the longitudinal equations of motion, primarily the pitch equations of motion. The uncoupled pitch dynamics consist of the pitching moment equation and the normal force equation. The longitudinal angular equation for pitch acceleration, or $\dot{q}$ is:

$$\dot{q} = M_\alpha \alpha + M_q q + M_{\delta e} \delta e \tag{4.1}$$

and the corresponding normal force equation is:

$$\dot{\alpha} = Z_\alpha \alpha + Z_q q + Z_{\delta e} \delta e \tag{4.2}$$

Combining equations 4.1 and 4.2 into a linear state-space model format gives:

$$\begin{bmatrix} \dot{\alpha} \\ \dot{q} \end{bmatrix} = \begin{bmatrix} Z_\alpha & Z_q \\ M_\alpha & M_q \end{bmatrix} \begin{bmatrix} \alpha \\ q \end{bmatrix} + \begin{bmatrix} Z_{\delta e} \\ M_{\delta e} \end{bmatrix} \delta e \tag{4.3}$$

The remainder of the research concentrates on solving for M_α, M_q and $M_{\delta e}$ from Equation 4.3 using the method of Linear Regression and comparing those results to "truth data" obtained from the simulation.

4.2 Linear Regression Method Validation

Before the experimental research began, the Linear regression method described in Chapter 2 was validated using the linear state-space model, Equation 4.3, with a simple set of longitudinal stability and control derivatives. This data was taken from Reference 8, for a small, single jet engine, military training airplane.

For an aircraft, the equations for the longitudinal dimensional stability derivatives (from Reference 8) are:

$$Z_\alpha = \frac{-\bar{q}S(C_{L_\alpha} + C_D)}{m} \tag{4.4}$$

$$Z_q = \frac{-\bar{q}S\bar{c}C_{L_q}}{2mU} \tag{4.5}$$

$$Z_{\delta e} = \frac{-\bar{q}SC_{L\delta e}}{m} \tag{4.6}$$

$$M_\alpha = \frac{\bar{q}S\bar{c}C_{m_\alpha}}{I_{yy}} \tag{4.7}$$

$$M_q = \frac{\bar{q}S\bar{c}^2 C_{m_q}}{2I_{yy}U} \tag{4.8}$$

$$M_{\delta e} = \frac{\bar{q}S\bar{c}C_{m\delta e}}{I_{yy}} \tag{4.9}$$

For the example aircraft, the following values were used to solve the above equations.

Flight condition:

25,000 ft. altitude, Mach 0.6, Cruise

Reference Geometry:

S (wing area) = 136 ft^2, $\bar{c}$ (root chord) = 4.4 ft

Flight Condition Data:

U (True Airspeed, TAS) = 610 ft/sec

$\bar{q}$ (Dynamic Pressure) = 198 lbs/ft^2

Mass Data:

W (weight) = 4,000 lb

$I_{yy} = 4,800$ slug-ft^2

Steady State Coefficients:

$C_L = 0.149$

$C_D = 0.0220$

Longitudinal Coefficients and Stability Derivatives (Stability Axis, Dimensionless):

$C_{L_\alpha} = 5.5$

$C_{Lq} = 10.0$

$C_{m_\alpha} = -0.24$

$C_{m_q} = -17.7$

Longitudinal Control and Hinge Moment Derivatives (Stability Axis, 1/rad)

$C_{L_{\delta e}} = 0.38$

$C_{m_{\delta e}} = -0.88$

Solving for Equations 4.4 through 4.9 and putting their values into Equation 4.3 gives,

$$\begin{bmatrix} \dot{\alpha} \\ \dot{q} \end{bmatrix} = \begin{bmatrix} -37.17 & -0.2979 \\ -290.82 & -2895.5 \end{bmatrix} \begin{bmatrix} \alpha \\ q \end{bmatrix} + \begin{bmatrix} -2.558 \\ -26.66 \end{bmatrix} \delta e \tag{4.10}$$

The linear state-space model was then simulated in MATLAB using the command

"LSIM" using a sine wave with amplitude of 100 as the control elevator input for 5

seconds. The resulting time histories for Angle of Attack, Pitch rate, Elevator deflection

and Pitch acceleration for the simulation are shown below in Figure 4-1.
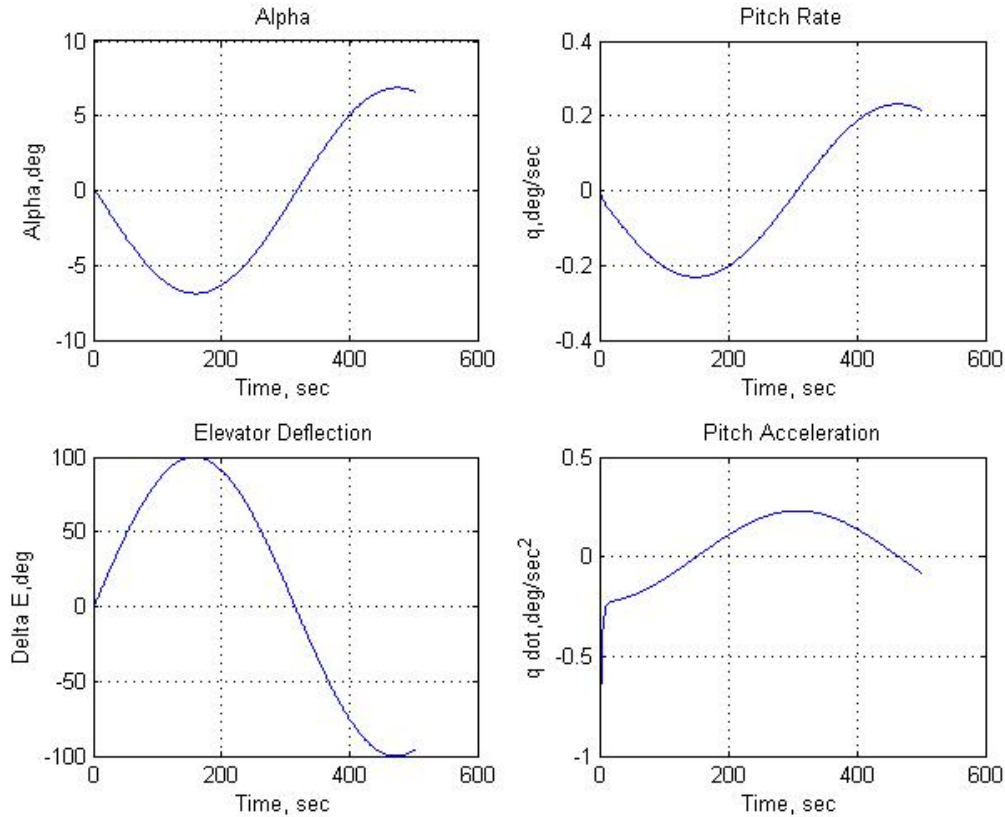
Figure 4-1 Time Histories of Linear model parameters

To validate the linear regression method described in Chapter 2, the time history values

of α (angle of attack in degrees), q (pitch rate in degrees/sec), δe (Elevator angle in

degrees) and $\dot{q}$ (pitch acceleration in degrees/sec^2) were obtained from the linear

simulation to estimate the derivatives, M_α, M_q and $M_{\delta e}$ using Equation 4.1.

$$\dot{q} = M_\alpha \alpha + M_q q + M_{\delta e} \delta e$$

Using Equation 2.9 from Chapter 2 for the least-squares estimator

$$\hat{\theta} = (X^T X)^{-1} X^T y$$

and defining X and Y as:

$$X = \begin{bmatrix} \alpha & q & \delta e \end{bmatrix} \qquad (4.11)$$

$$Y = \dot{q} \qquad\qquad (4.12)$$

The values obtained for $\hat{\theta}$ using Equation 4.11, 4.12 and 2.9 are compared to the original

values calculated from Equations 4.4 through 4.9 in Table 4-1 below.

Table 4-1: Comparison of Longitudinal Dimensional Stability Derivatives

	Θ Values	"Truth Data" (Equations 4.4 – 4.9)
Mα	-290.8	-290.82
Mq	-2895.5	-2895.5
Mδe	-26.70	-26.66

From Table 4-1, it is shown that the linear regression method produces results that

compare well with "Truth Data". Slight variations in the numbers are due to rounding in

MATLAB. This validates the method for the scope of this research.

4.3 Exercising the Simulation

The 6-DOF missile simulation described in Chapter 3 was exercised to create a

series of batch runs containing several different missile fly-out scenarios terminating

when the missile reached the target. After reviewing the accumulated data from the

simulation, it was found that the autopilot of the missile model was not commanding a

suitable input for excitation of missile maneuvers used for parameter identification.

4.3.1 Control Signal Input Form

Determining the best input form to successfully excite the missile airframe for

parameter identification study is one of the most critical parts of the design of the

experiment. Many different forms of control inputs have been used. There are usually four common kinds:

- Transient (Step, Impulse etc.)

- Sinusoids of various frequencies and amplitudes (Doublets)

- Stochastic signals

- Pseudorandom (white) noise

It is well known that the shape of an input signal could influence the accuracy of estimated parameters from dynamic flight measurements.[9]

The power of an input signal should be distributed uniformly over the frequency range covering the dominant airframe dynamics. Transient signals such as a step input or an impulse usually fail in this regard due to their short duration over the simulation. All modes of the system might not be excited (lack of persistent excitation) and the regressor matrices used to obtain model parameters might be close to being singular leading to numerical problems. In Figure 4-1 taken from Reference 9, power spectral densities of three inputs are presented. The step input excites modes of lower frequencies only, which makes it unsuitable for parameter estimation. The power spectral density of a multi-step input is a relatively wide band compared to the doublet, which excites only a particular band at a higher frequency. By changing the duration of the doublet, the peak of the power spectral density can be shifted to lower or higher frequencies, which makes it very suitable for parameter estimation.

System identification using pseudorandom noise signals is also very commonly used. The noise is usually rich in all frequencies and therefore excites all modes of the plant being measured. This leads to good estimates of the model parameters.[10]
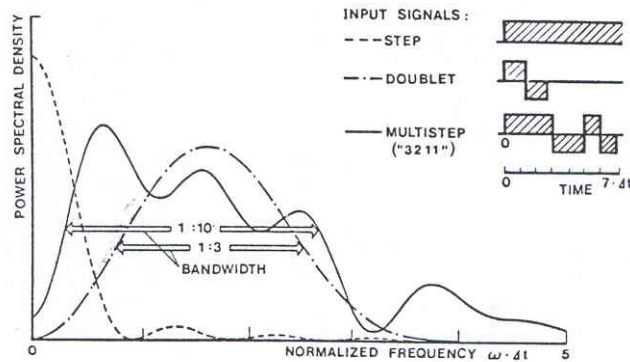
Figure 4-2 Frequency Domain Comparison of Various Input Signals

Klein, Reference 9, has determined other basic requirements for aircraft parameter identification:

- The input form should be selected in agreement with the mathematical model representing the aircraft under test. For example, an input for the longitudinal short-period model with linear stability and control derivatives should not cause aircraft motion where the assumptions of constant airspeed and linear aerodynamics are not valid.

- The input form should also be within the bandwidth of the actuator driving the control surface being commanded for the maneuver of the missile. The missile model used for this research does not have an actuator modeled; the commanded input is directly fed through to the model without being augmented by actuator dynamics. Therefore, this requirement and the implications associated with it were not included in the scope in this research.

It was decided, based on the results of the original simulation runs, to by-pass the autopilot in the simulation with a command generator utilizing a series of different pitch doublets varying in frequency including band-limited white noise. After testing multiple inputs of pitch doublets and band-limited white noise of varying frequencies and

amplitudes, two input types showed the most potential to be used for the estimation of the longitudinal derivatives of the missile. These input types were chosen because they provided the most excitation to the system without exceeding the physical limitations of missile actuator hardware. The first input type is a pitch doublet at 2 Hz, shown in Figure 4-3. The second input type is band-limited white noise that produces a normally distributed random signal, shown in Figure 4-4.
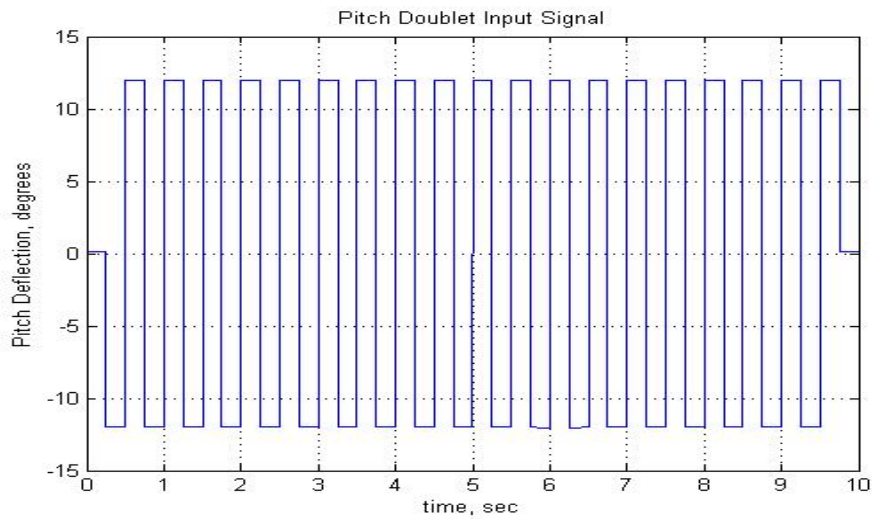

Figure 4-3 Two Hz Pitch Doublet Input Signal
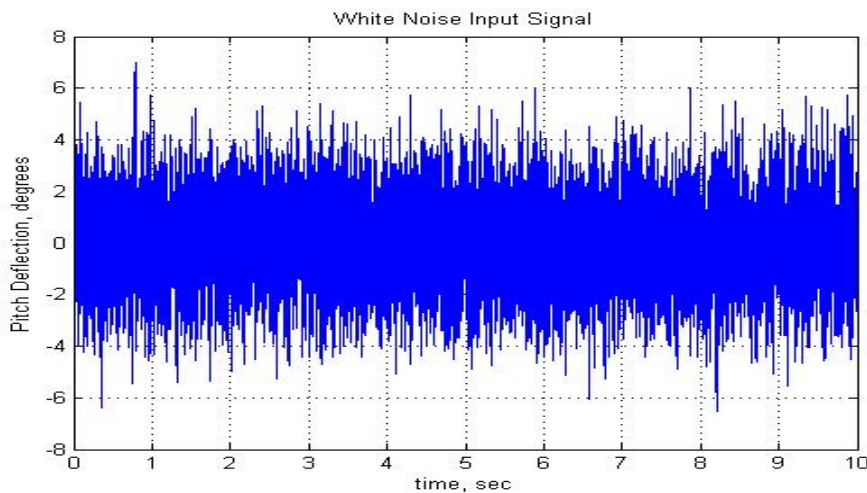
Figure 4-4 Band-Limited White Noise Input Signal

4.3.2 Control Signal Input Implementation into Simulation

The missile is modeled in the cruciform shape (PHIPRM = 0.0) having 4 different

control surfaces along the X and Y-axis as seen in Figure 4-5.
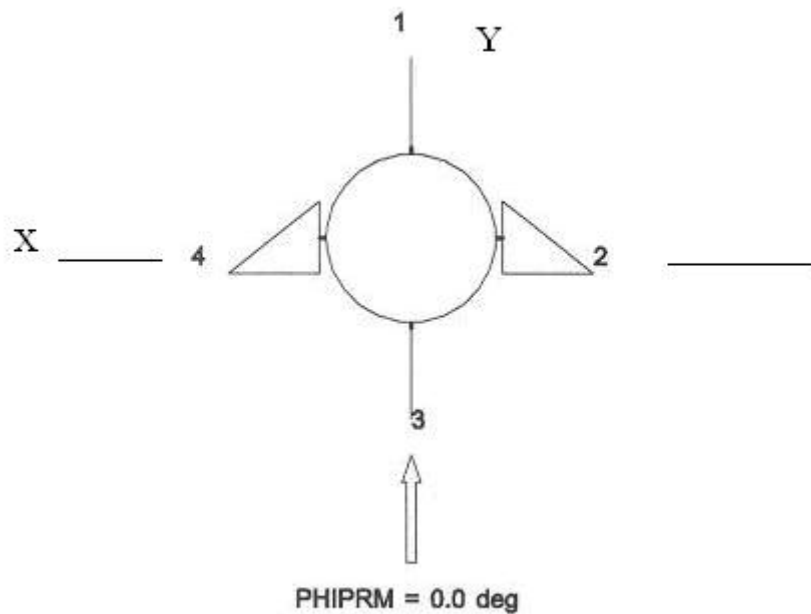
Figure 4-5 Cruciform Missile Layout

The relationship between the individual control deflections and three axes control

deflections is shown from Equation 3.10, repeated here.

$$\begin{bmatrix} \delta 1 \\ \delta 2 \\ \delta 3 \\ \delta 4 \end{bmatrix} = \begin{bmatrix} 1 & \sin\phi & -\cos\phi \\ 1 & \cos\phi & \sin\phi \\ 1 & -\sin\phi & \cos\phi \\ 1 & -\cos\phi & -\sin\phi \end{bmatrix} \begin{bmatrix} \delta P \\ \delta Q \\ \delta R \end{bmatrix}$$

Fins numbered 2 and 4 are the pitch control surfaces and Fins 1 and 3 control the roll

and yaw axes. Fins 2 and 4 are coupled together with Fin 4 commanding opposite that of

Fin 2. This equates to a negative command input for Fin 4 in the simulation. Since this

research focused only on the determining the longitudinal stability and control derivatives, Fins number 2 and 4 were commanded with the pitch command inputs described in Figures 4-3 and 4-4 above and Fins numbered 1 and 3 were set to zero.

4.4 Linear Regression Estimation

The data was collected by running the simulation twice; each instance using one of the two input signals selected from Section 4.3. The High frequency pitch doublet in Figure 4-3 will be labeled Test Case 1 and the Band limited white noise signal in Figure 4-4 will be labeled Test Case 2. The variables, α (angle of attack in degrees), q (pitch rate in degrees/sec), δe (Elevator angle in degrees) and $\dot{q}$ (pitch acceleration in degrees/sec^2) were collected from the simulation time history for the research. They are as follows for Test Case 1 and Test Case 2, respectively.
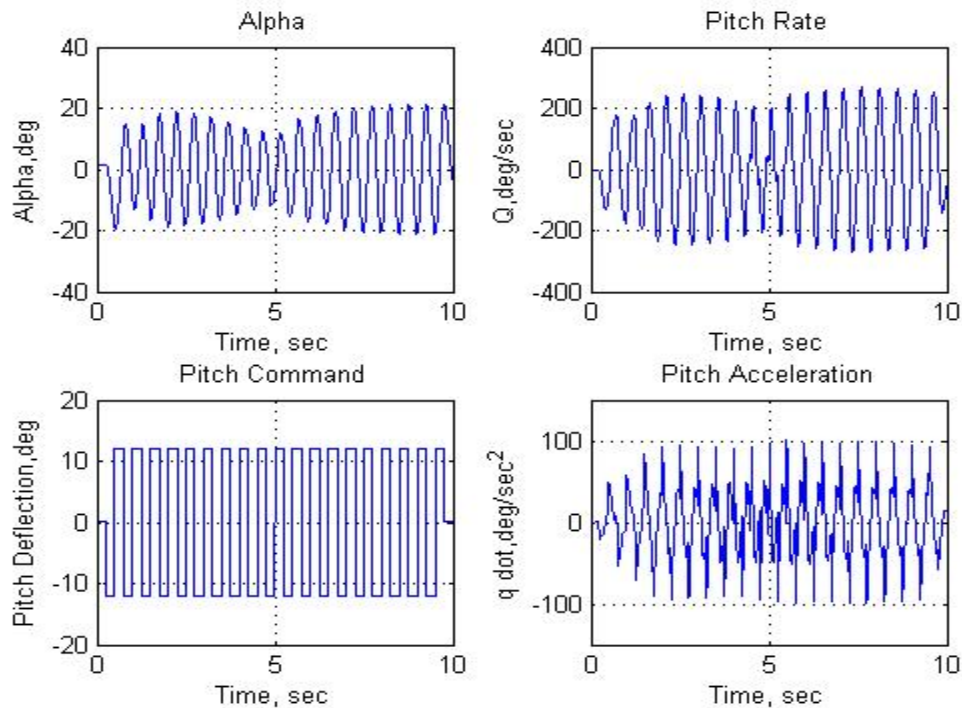
Figure 4-6 High Frequency Pitch Doublet Input/Output (Test Case 1)

68
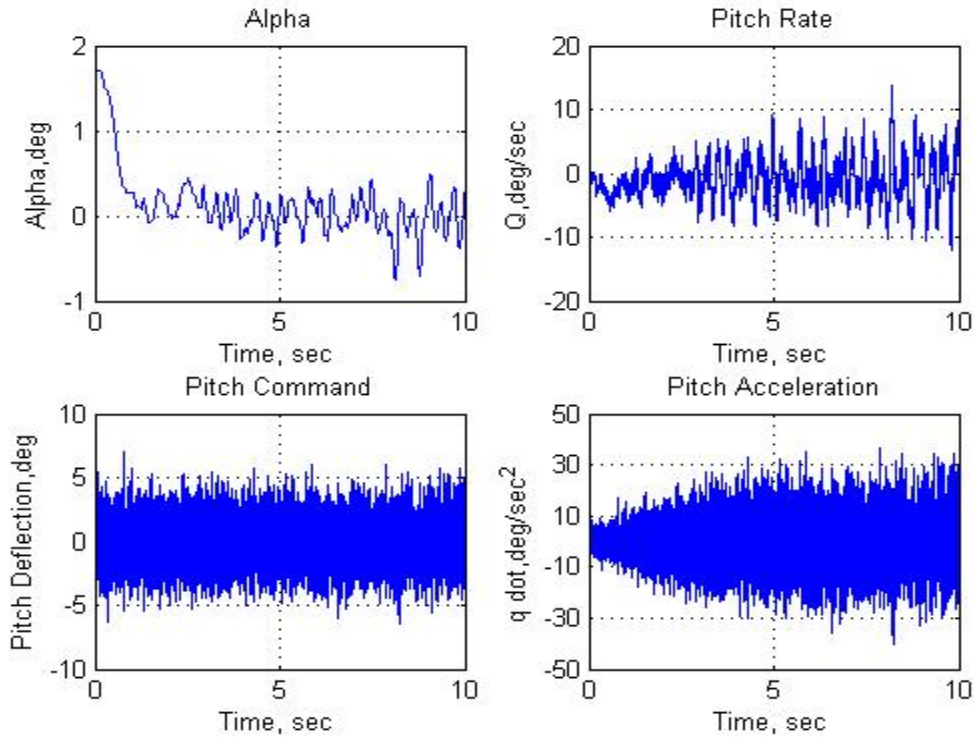
Figure 4-7 Band Limited White Noise Input/Output (Test Case 2)

Data collected from each simulation time history was partitioned into discrete samples

taken at every 10th sample, or every 0.01 seconds for the entire time of the simulation,

which ran for 10 seconds with 10,000 samples taken. The time histories were partitioned

in this way for the estimation of the longitudinal dimensional stability derivatives, M_α,

M_q and $M_{\delta e}$.

These derivatives are computed by utilizing the Linear regression technique, described in

Chapter 2, to solve Equation 4.1 from Section 4.2

$$\dot{q} = M_\alpha \alpha + M_q q + M_{\delta e} \delta e$$

Using Equation 2.9 from Chapter 2 for the least-squares estimator

$$\hat{\theta} = (X^T X)^{-1} X^T y$$

Where X, also called the regressor matrix, and Y are defined as:

$$X_1 = \begin{bmatrix} \alpha & q & \delta e \end{bmatrix} \tag{4.13}$$

$$Y = \dot{q} \tag{4.14}$$

Partitioning the data to every 10 samples satisfies the requirement that $m \geq n$ in order to estimate the n parameters for θ_i, where $m = 10$ and $n = 3$. From Equation 2.4,

$$y = \begin{bmatrix} y(1) \\ y(2) \\ y(3) \\ \vdots \\ y(m) \end{bmatrix} \quad X = \begin{bmatrix} x_1(1) & \cdots & x_n(1) \\ x_1(2) & \cdots & x_n(2) \\ \vdots & & \vdots \\ x_1(m) & \cdots & x_n(m) \end{bmatrix} \quad \theta = \begin{bmatrix} \theta_1 \\ \theta_2 \\ \vdots \\ \theta_n \end{bmatrix}$$

Solving Equation 2.9 gives a θ at each partitioned sample data set where:

$$\theta_1 = \begin{bmatrix} M_\alpha & M_q & M_{\delta e} \end{bmatrix} \tag{4.15}$$

Figures 4-8 through 4-19, which will be discussed in the following section, show the comparison between the estimated values of M_α, M_q and $M_{\delta e}$ to the actual values from the 6-DoF missile model simulation. Some of the Figures show the effect of passing the data through a second-order filter, given by:

$$Filter = \frac{\omega_n^2}{s^2 + 2\zeta\omega_n s + \omega_n^2} \tag{4.16}$$

Where,

$$\omega_n = 2\pi \cdot 2 \qquad \text{and} \qquad \zeta = \frac{\sqrt{2}}{2} \tag{4.17}$$

These filtered estimates are shown in Figures 4-11, 4-15 and 4-19 for Test Case 1 and Figures 4-13, 4-17 and 4-21 for Test Case 2.

4.4.1 Linear Regression Estimation Analysis of Results

This section presents an analysis of the results obtained from applying the Linear Regression method to estimate the longitudinal stability and control derivatives from the simulation truth data.

4.4.1.1 M_α, Pitch angular acceleration per unit angle of attack:

Figures 4-10 and 4-11 show the estimates of M_α for Test Case 1 compared to the truth data from the simulation. Once the estimate data was filtered, it was easier to see the trend of the data for each estimate. The overall trend is good, however there is some bias in the estimate data. Figures 4-12 and 4-13 show the estimates of M_α for Test Case 2 compared to the same truth data from the simulation. The filtered data shown in Figure 4-13 show that for the time history captured, the estimate follows well with the trend with very little bias. While the estimate doesn't exactly track the oscillations of the truth data, the overall mean values compare well, based on a visual inspection of the figure. Overall, results obtained for M_α were better with the band-limited white noise command signal input than the pitch doublet.

4.4.1.2 M_q, Pitch angular acceleration per unit pitch rate:

Figures 4-14 and 4-15 show the estimates of M_q for Test Case 1 compared to the truth data from the simulation. Again, it was easier to see the trend of the data using the filtered estimate. The estimate had an average bias of about 0.2 compared to the truth data and had some erratic data points in the estimate near end of the time history. These erratic data points at the end are cause by an ill-condition X matrix for the estimates at

this time section. This will be further discussed later in this report. Figures 4-16 and 4-17 show the estimates of M_q for Test Case 2 compared to the same truth data from the simulation. The filtered data shown in Figure 4-17 show that for the time history captured, the had an average bias of about 0.2, identical to Test Case 1. Overall, both Test Cases failed to estimate M_q with any real accuracy. This was expected, however, because M_q is generally difficult to estimate with parameter ID techniques.

4.4.1.3 $M_{\delta e}$, Pitch angular acceleration per unit elevator (pitch deflection) input:

Figures 4-18 and 4-19 show the estimates of $M_{\delta e}$ for Test Case 1 compared to the truth data from the simulation. From the filtered estimate data, it was easier to see the trend of the data for each estimate. The overall trend is good; there is little overall bias in the data with the exception to the erratic data points found in the data near the beginning and at the end of the time history. These erratic data points result from ill-conditioned regressor matrices, X , which will soon be discussed.

Figures 4-20 and 4-21 show the estimates of $M_{\delta e}$ for Test Case 2 compared to the same truth data from the simulation. The filtered data shown in Figure 4-21 shows that for the time history captured, the estimate follows well with the trend of the truth data. There is, however, a small horizontal shift in the data compared to the un-filtered estimate data in Figure 4-20. This shift or bias is caused by the second order filter implemented to smooth the original estimate data. If the truth data is also filtered with the second order filter the shift goes away. This is seen in Figure 4-22. Overall, results obtained for $M_{\delta e}$ were better with the band-limited white noise command signal input

than the pitch doublet. This next section will discuss what an ill-conditioned regressor

matrix is and how it is determined.

4.4.1.4 Condition number of Regressor Matrix, X_1

The condition number of a matrix provides an indication of the sensitivity of the

solution of a system of linear equations to errors in the data. The 2-norm condition of a

rectangular matrix is the ratio of the largest and smallest singular values. For rectangular

matrices with full column rank:

$$X \in IR^{mxn}, rank(X) = n \Rightarrow \kappa(X) = \frac{\sigma_{max}(X)}{\sigma_{min}(X)} \tag{4.18}$$

It gives an indication of the accuracy of the results from matrix inversion and the

linear equation solution. Values near 1 indicate a well-conditioned matrix. Large

condition numbers indicate a nearly singular matrix or an ill-conditioned matrix. Figures

4-8 and 4-9 give the condition number of the estimates, θ_1 for the regressor matrix, X_1 for

both Test Case 1 and Test Case 2. The highest and lowest condition numbers for both

commanded signal input types for X_1 are shown in Table 4-2 below.

Table 4-2: Comparison of Maximum and Minimum Condition Numbers for X_1

Regressor Matrix, X_1	Highest Condition Number	Lowest Condition Number
Test Case 1	$3e^6$	$3e^3$
Test Case 2	$5e^3$	10
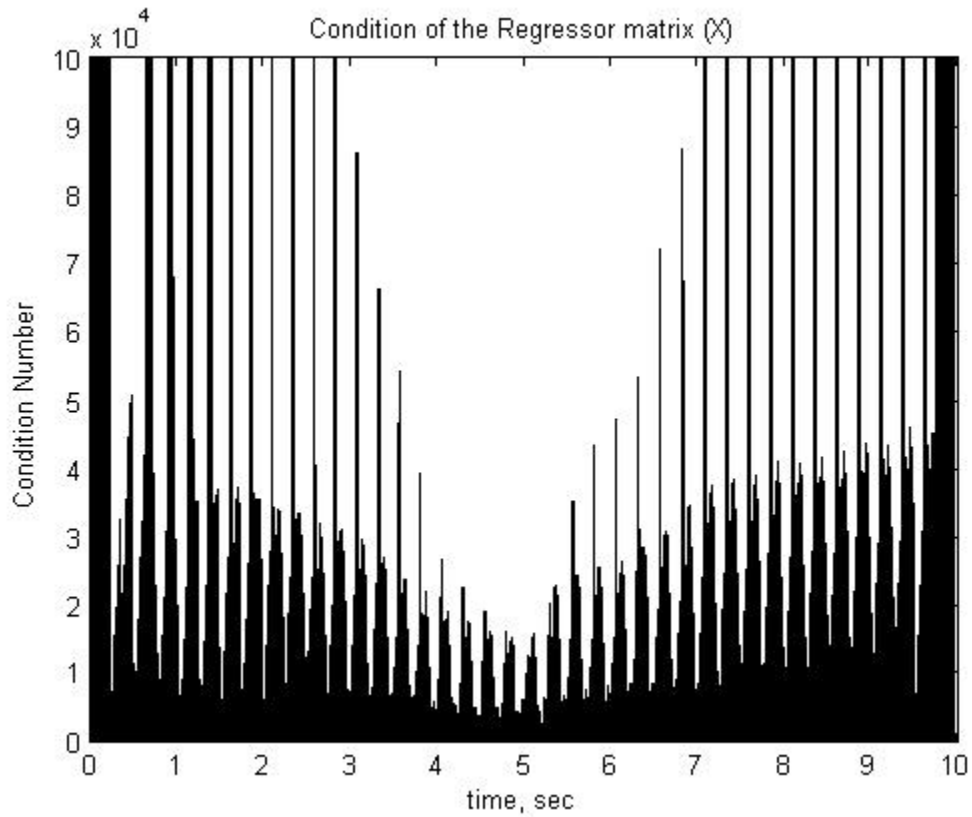
Figure 4-8 Condition Number of X_1 for Test Case 1
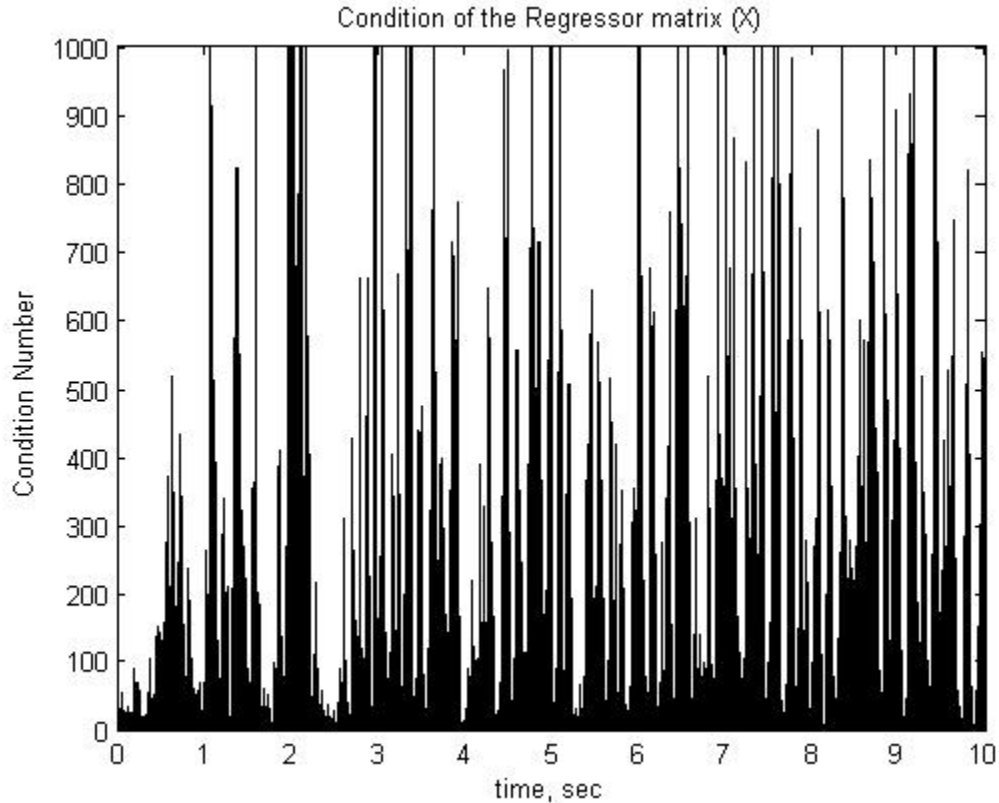
Figure 4-9 Condition Number of X$_1$ for Test Case

From observation of Figure 4-9, high condition numbers occur at the beginning and the end of the time history data set. This has a direct correlation to the shape of the estimates of M_α, M_q and $M_{\delta e}$ for Test Case 1 in Figures 4-11, 4-15 and 4-19, where the erratic data points in the beginning and end of the time history exist. This indicates that the pitch doublet signal used for Test Case 1 was not set to a high enough frequency to excite all the modes of the system, which therefore, produces the singularities in the Regressor Matrix, X. These singularities also occur when the commanded pitch signal crosses zero in the simulation.

Figure 4-9 shows an average condition number for Test Case 2 for the entire time history. This trend could translate into the biases seen in Figures 4-13, 4-17 and 4-21 for

75

the estimates for Test Case 2. From Figures 4-8 and 4-9, it is clear that the band-limited

white noise signal does a better job of exciting the modes of the system than the pitch

doublet due to the lower condition numbers (fewer singularities) shown in Figure 4-9.
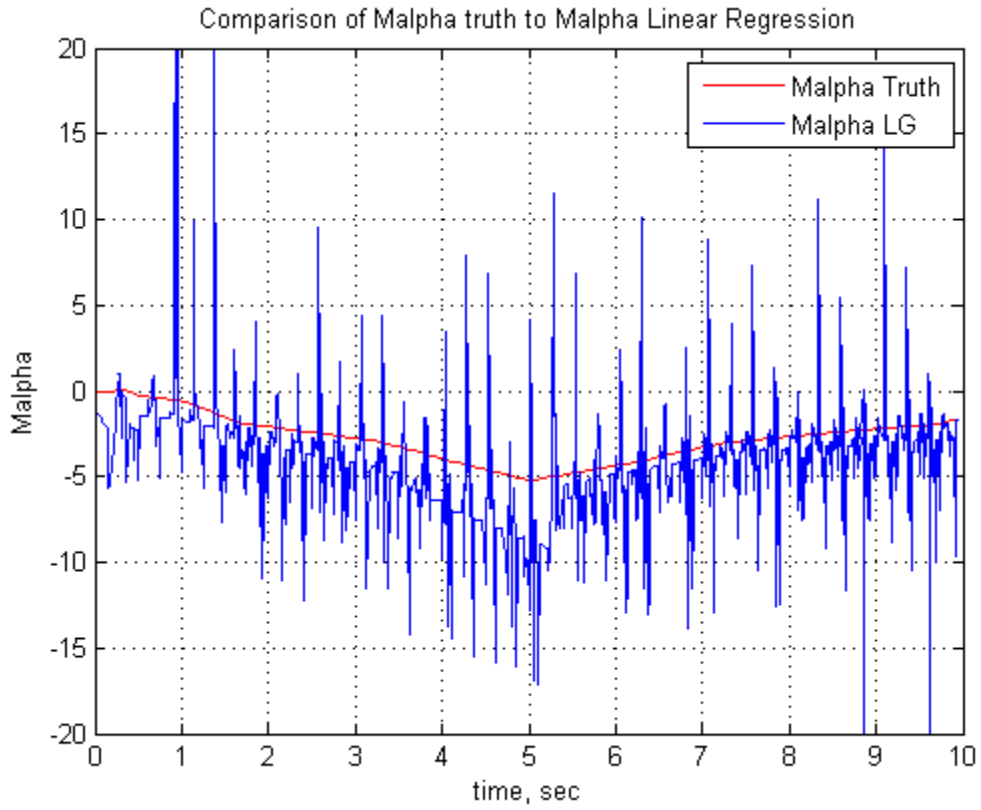
Figure 4-10 Test Case 1 Comparison of θ_1 to "Truth Data" for M_α
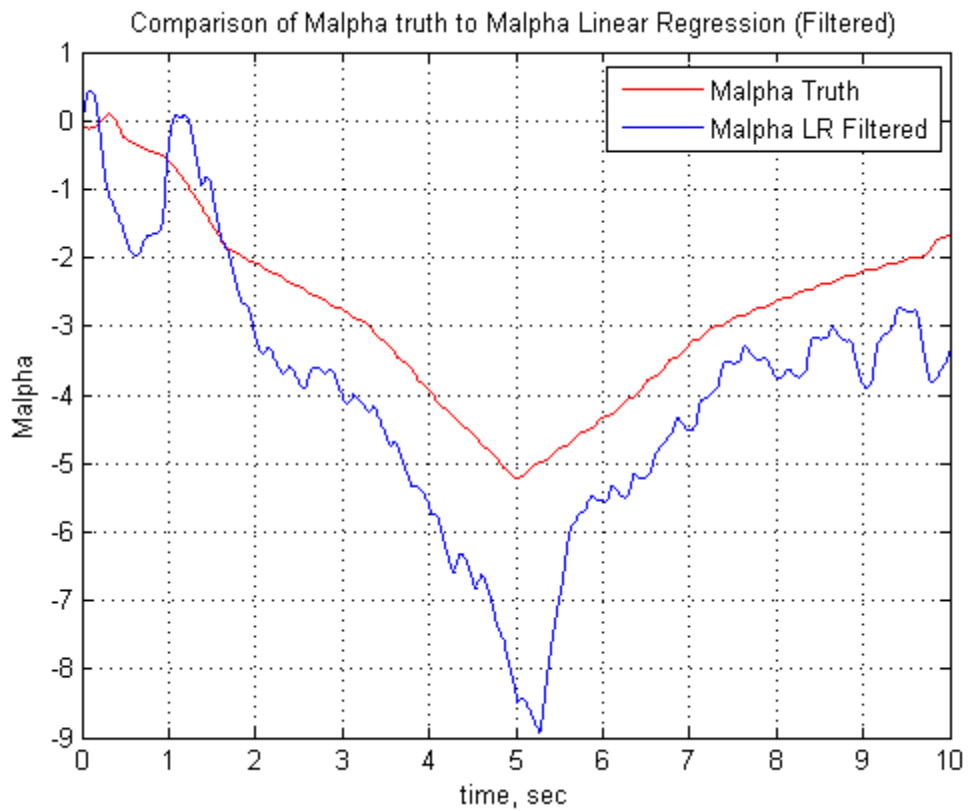
Figure 4-11 Filtered Test Case 1 Comparison of θ_1 to "Truth Data" for M_α
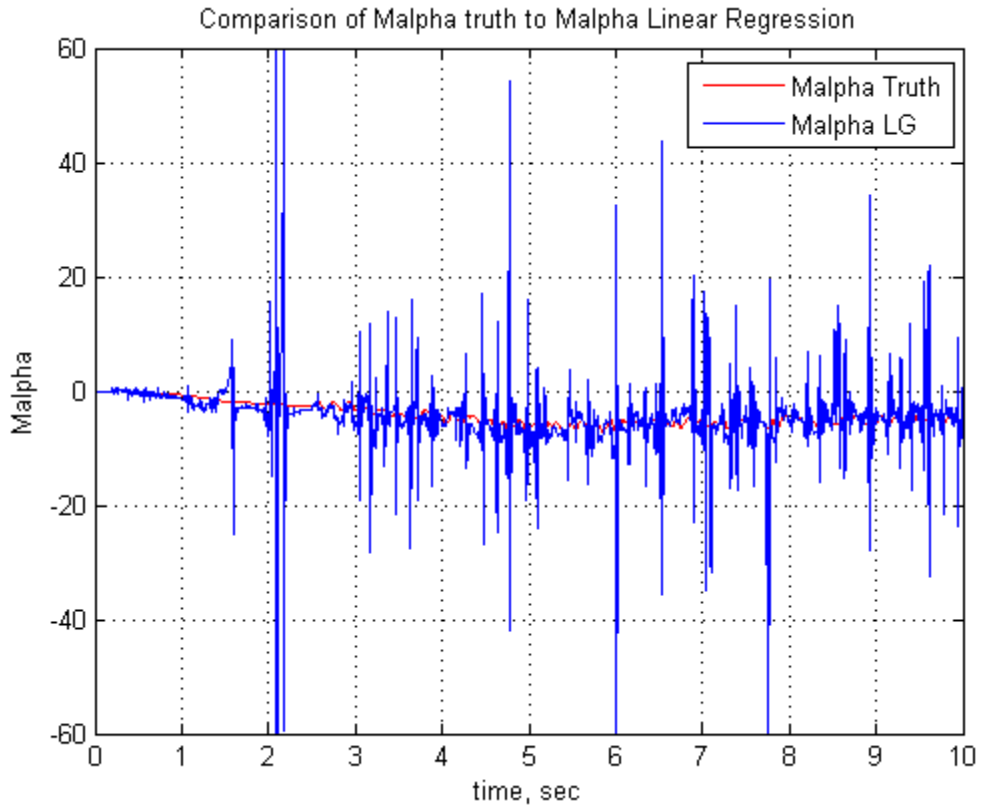
Figure 4-12 Test Case 2 Comparison of θ_1 to "Truth Data" for M_α
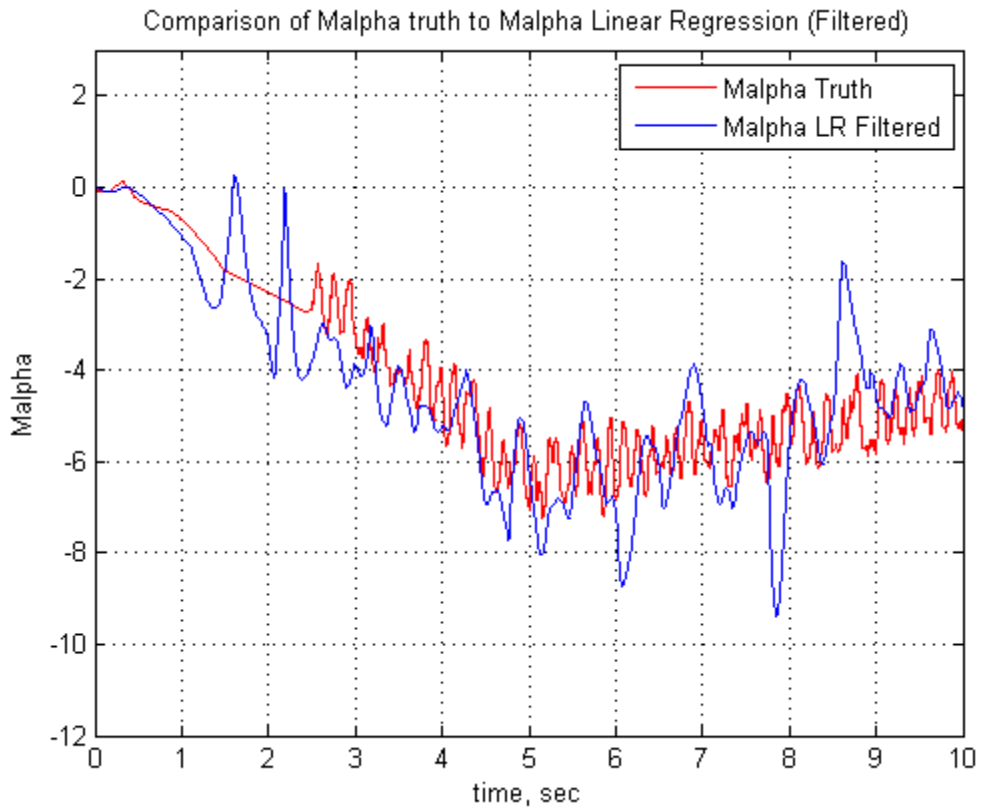
Figure 4-13 Filtered Test Case 2 Comparison of θ_1 to "Truth Data" for M_α
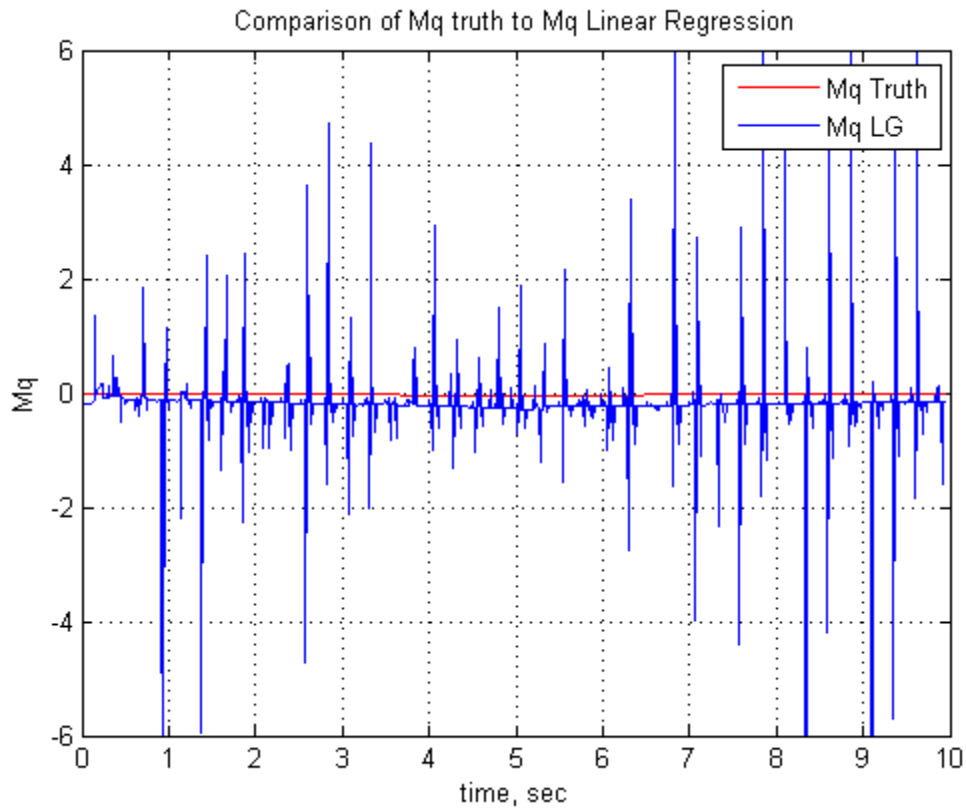
Figure 4-14 Test Case 1 Comparison of θ_1 to "Truth Data" for M_q
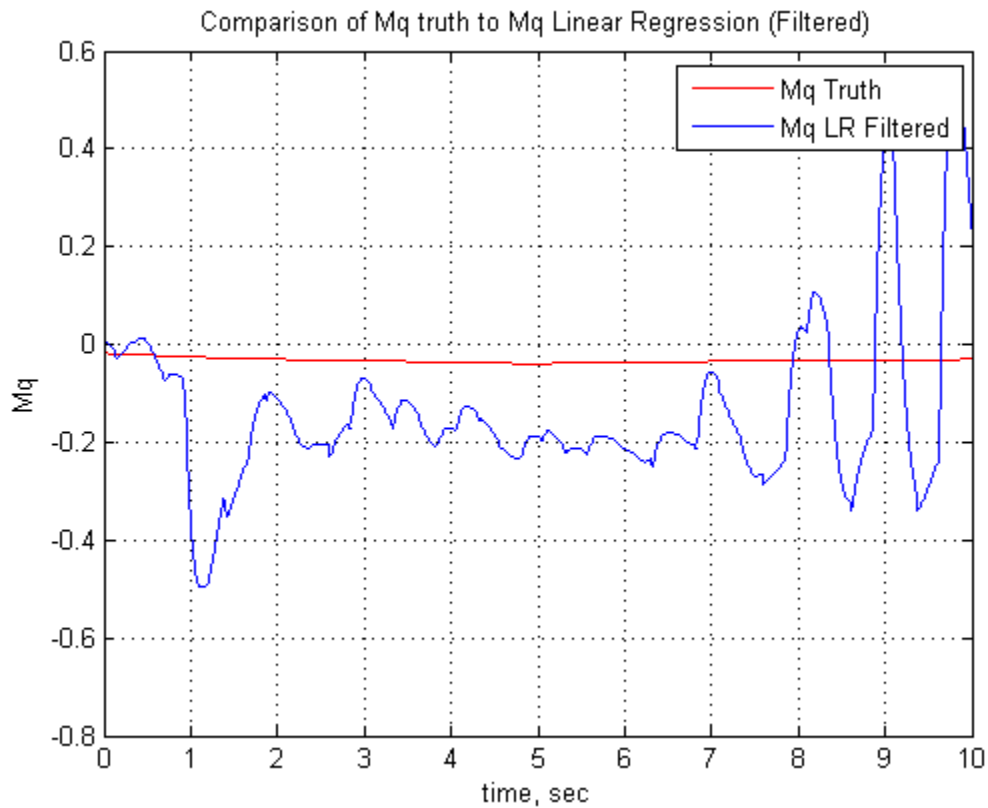
Figure 4-15 Filtered Test Case 1 Comparison of θ_1 to "Truth Data" for M_q
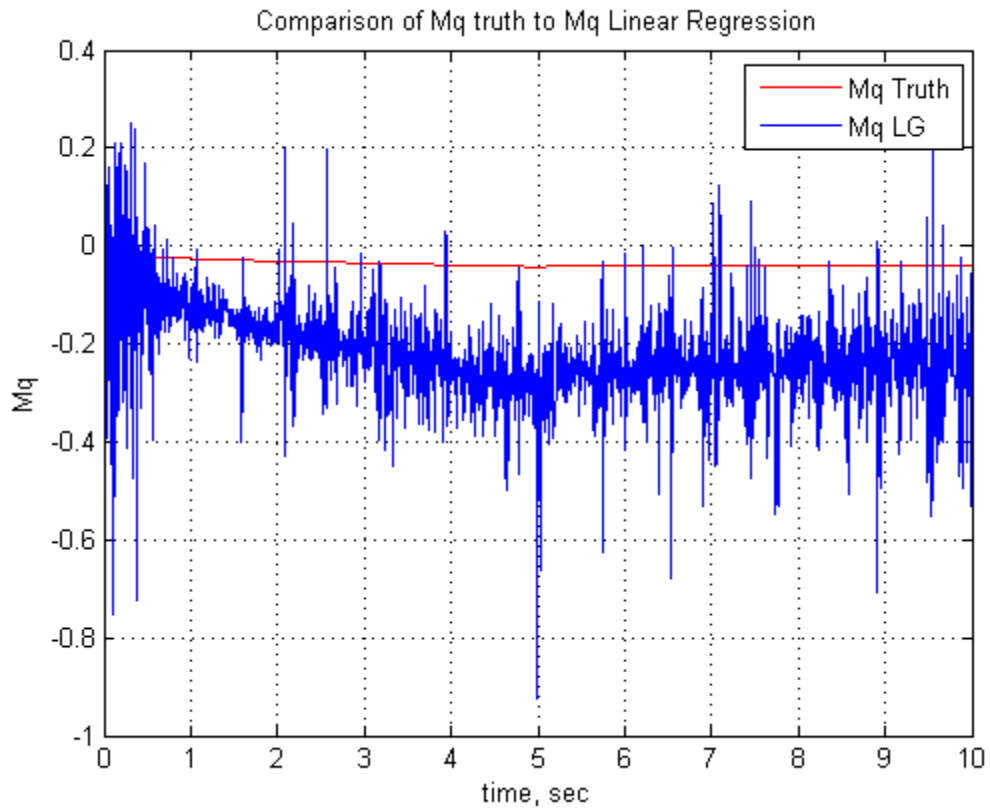
Figure 4-16 Test Case 2 Comparison of θ_1 to "Truth Data" for M_q
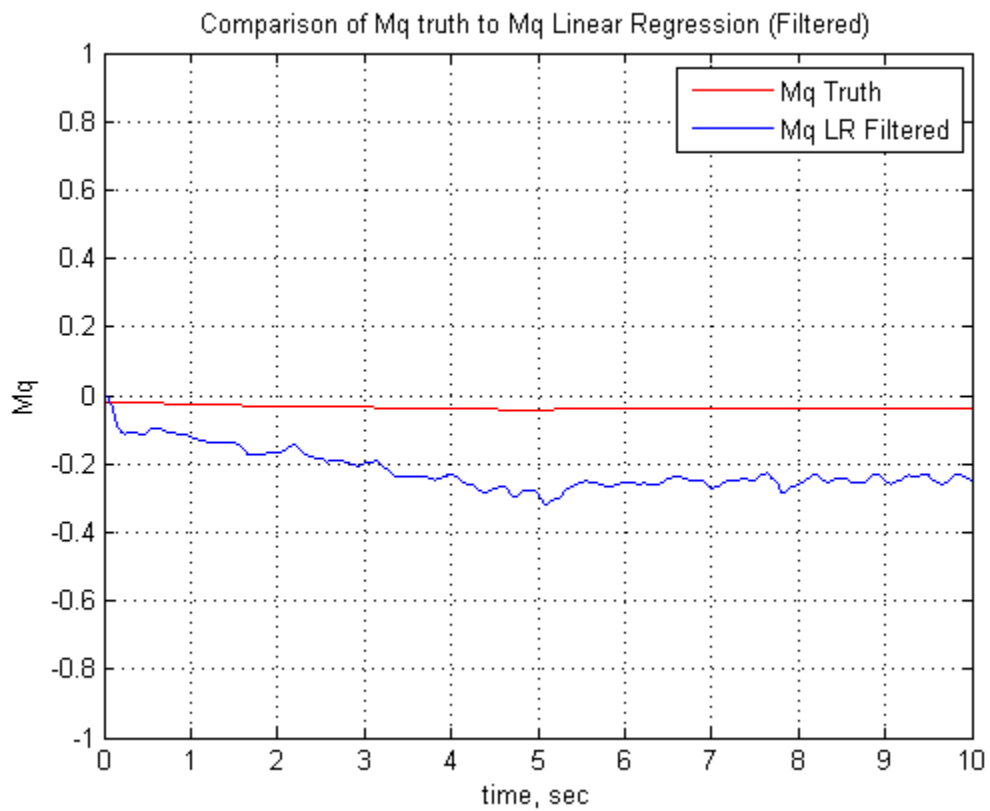
Figure 4-17 Filtered Case 2 Comparison of θ_1 to "Truth Data" for M_q
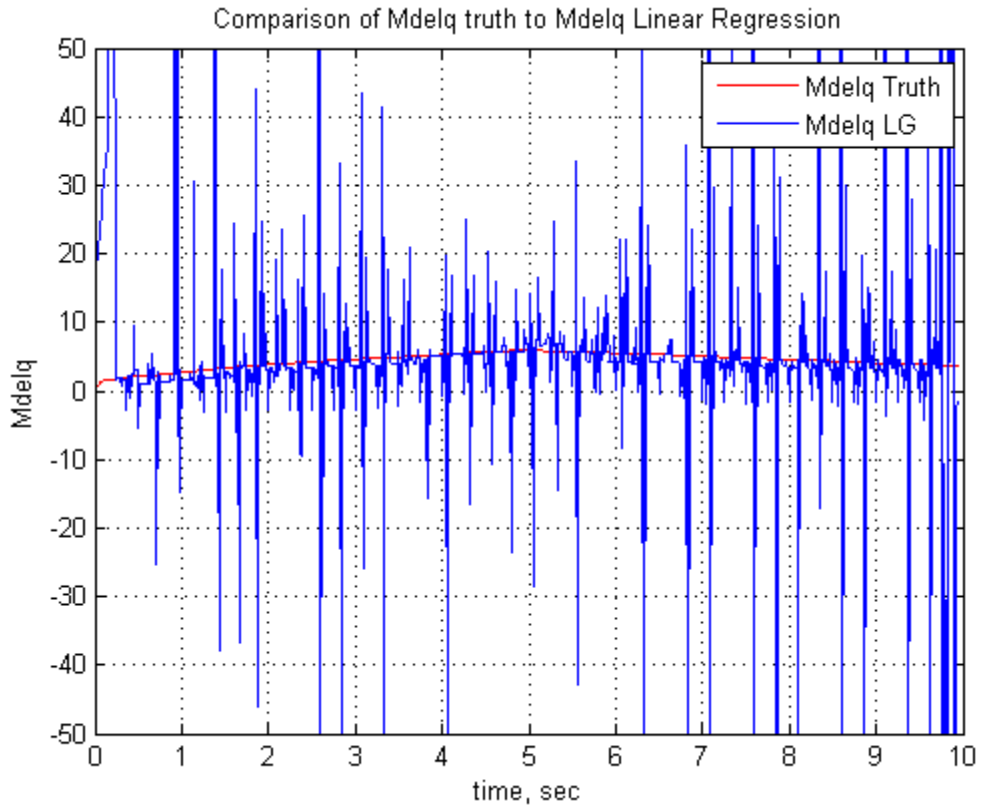
Figure 4-18 Test Case 1 Comparison of θ_1 to "Truth Data" for $M_{\delta e}$
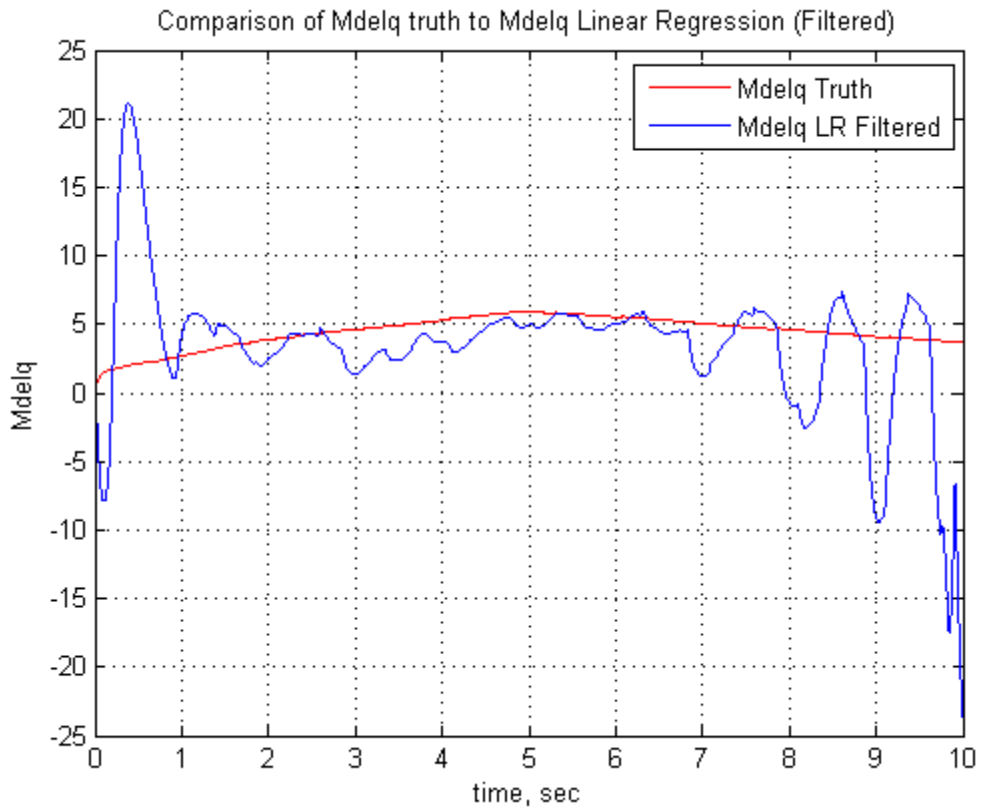
Figure 4-19 Filtered Test Case 1 Comparison of θ_1 to "Truth Data" for $M_{\delta e}$
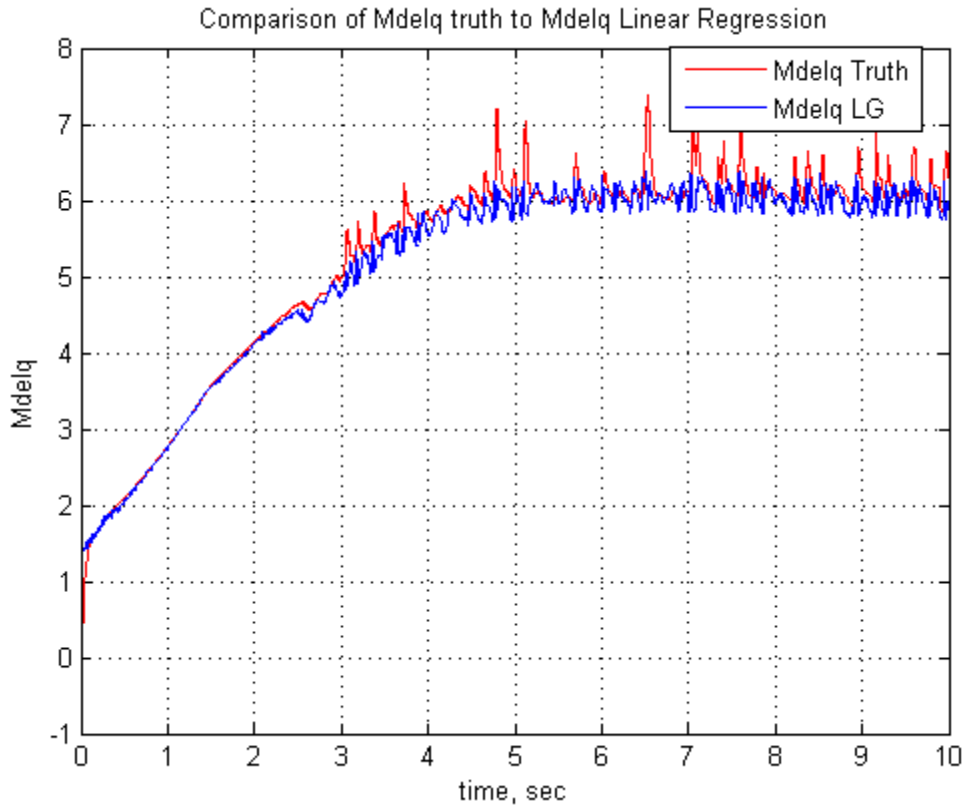
Figure 4-20 Test Case 2 Comparison of θ_1 to "Truth Data" for $M_{\delta e}$
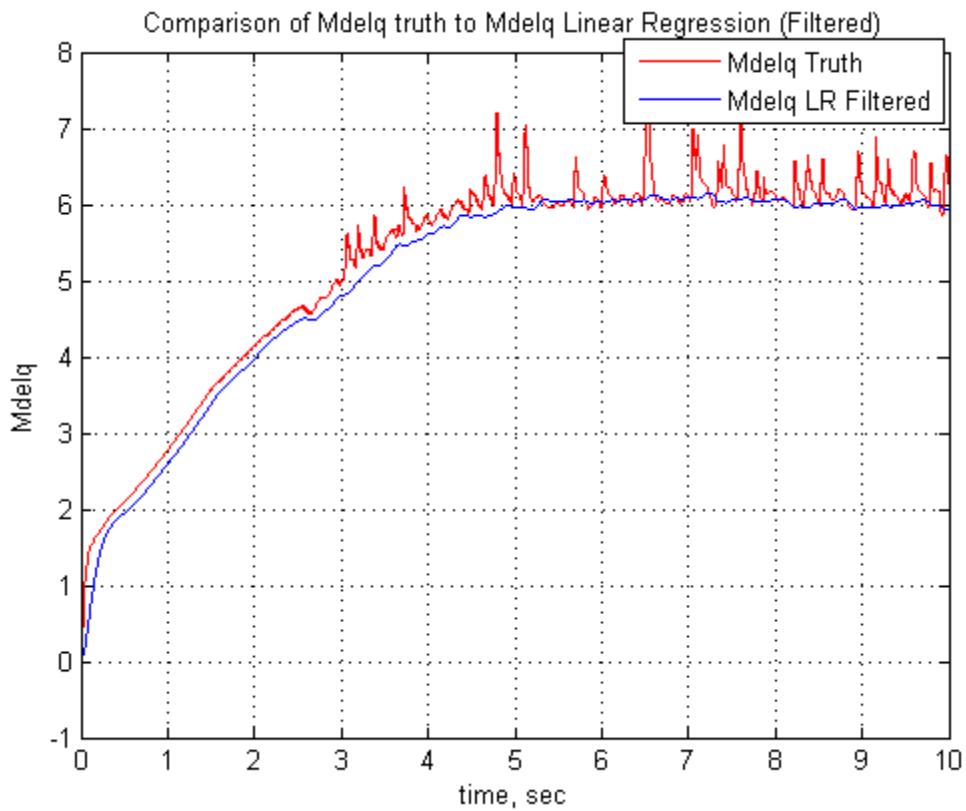
Figure 4-21 Filtered Test Case 2 Comparison of θ_1 to "Truth Data" for $M_{\delta e}$

82

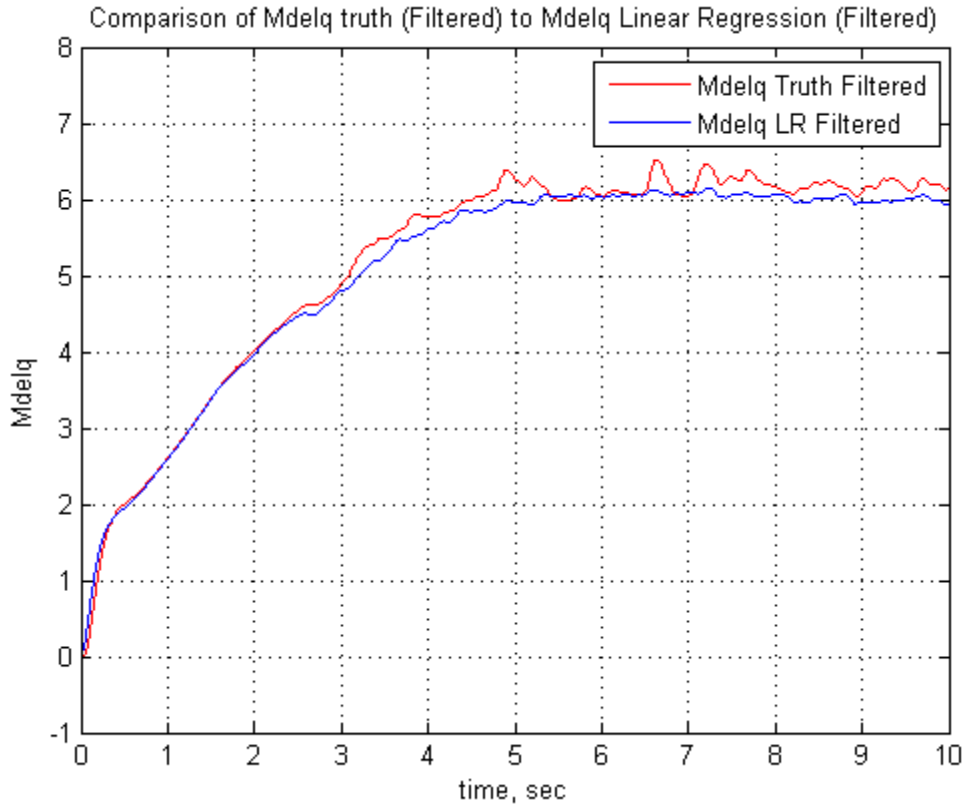Comparison of Mdelq truth (Filtered) to Mdelq Linear Regression (Filtered)

Figure 4-22 Comparison of Filtered Est. to Filtered Truth Data

4.5 Linear Regression Estimation Validation

The next step of the research focused on examining the validity of the calculated

estimates for M_α, M_q and $M_{\delta e}$. To test this, the time histories of the estimates, θ_1

were fed into the linear model of the system, from Equation 4.3:

$$\begin{bmatrix} \dot{\alpha} \\ \dot{q} \end{bmatrix} = \begin{bmatrix} Z_\alpha & Z_q \\ M_\alpha & M_q \end{bmatrix} \begin{bmatrix} \alpha \\ q \end{bmatrix} + \begin{bmatrix} Z_{\delta e} \\ M_{\delta e} \end{bmatrix} \delta e$$

Where:

$$Z_\alpha = \frac{l}{c} \cdot M_\alpha \tag{4.19}$$

$$Z_q = \frac{l}{c} \cdot M_q \tag{4.20}$$

$$Z_{\delta_e} = \frac{l}{c} \cdot M_{\delta_e} \tag{4.21}$$

Where, $l = 0.4696\,\text{m}$ (missile length) and $c = 0.1280\,\text{m}$ (missile diameter).

This linear model was then simulated in SIMULINK in discrete time, using the same command inputs as for the 6-DoF missile model simulation (from Figures 4-3 and 4-4) and the output data was recorded. Once again, the variables α (angle of attack in degrees), q (pitch rate in degrees/sec), δe (Elevator angle in degrees) and $\dot{q}$ (pitch acceleration in degrees/sec^2) were collected from the simulation time history for the research. These time histories for both Test Case 1 and Test Case 2 are shown below in Figures 4-23 and 4-24.
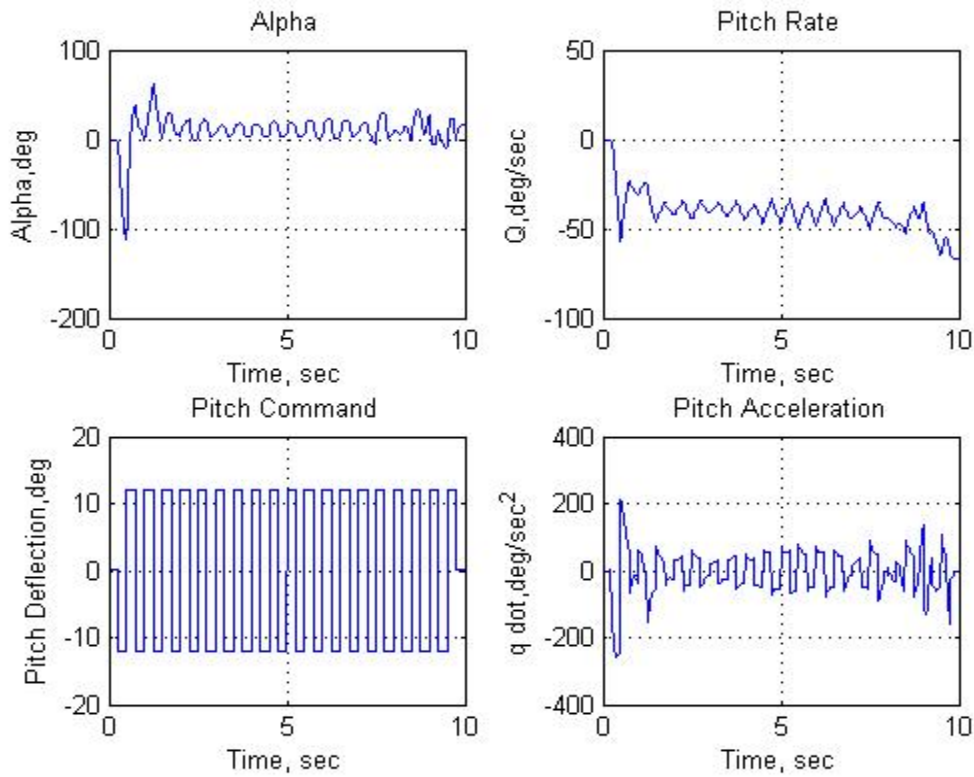
Figure 4-23 Pitch Doublet Input/Output for Linear Model (Test Case 1)
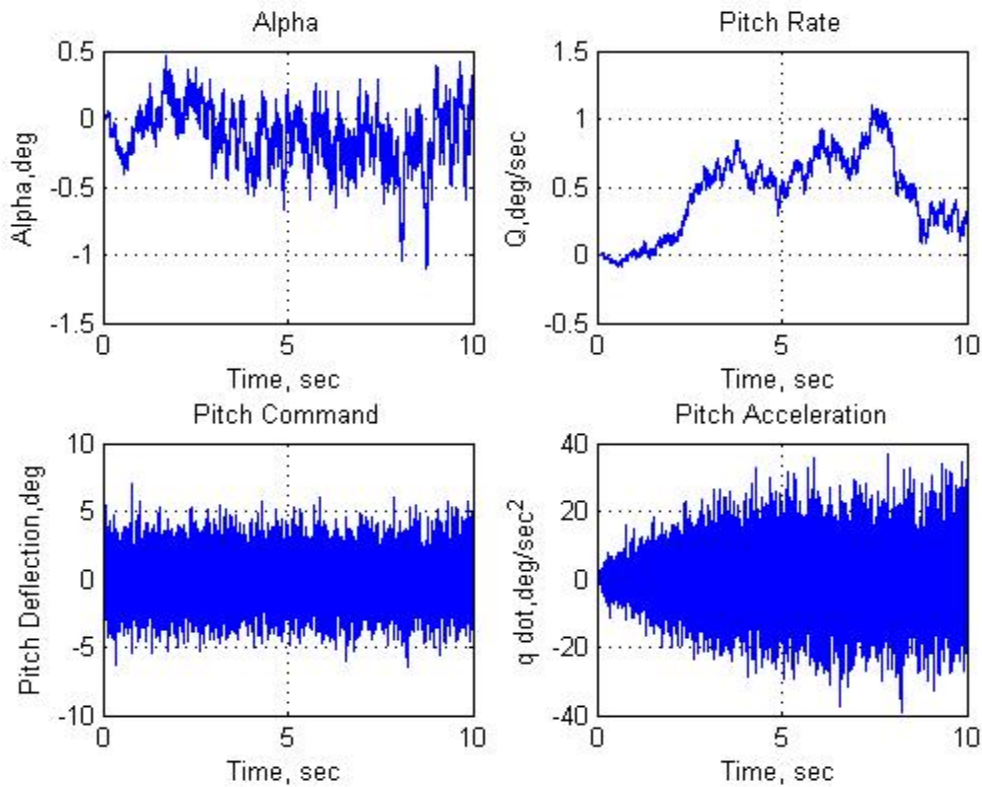

Figure 4-24 White Noise Input/Output for Linear Model (Test Case 2)

The derivatives, M_α, M_q and $M_{\delta e}$ were then estimated for a second time from the time history outputs of the linear model in Equation 4.3 with the original estimates acting as the truth states of the model.

The original estimates θ_1 were compared to the new estimates of the linear model, θ_2 to check the estimation technique. The new estimates θ_2 were filtered using Equations 4-14 and 4-15 and were compared to the original estimates made from the 6-DoF missile model simulation. Figures 4-27 through 4-32 shows the comparisons made between the original estimate, θ_1 to the linear model estimate, θ_2 for both Test Case 1 and Test Case 2.

4.5.1 Linear Regression Estimation Validation Analysis of Results

This section presents an analysis of the results obtained from applying the Linear Regression method to estimate the longitudinal stability and control derivatives from the simulation truth data.

4.5.1.1 M_α, Pitch angular acceleration per unit angle of attack:

Figure 4-27 shows the estimates, θ_2 of M_α for Test Case 1 compared to the original estimates, θ_1. The overall trend did not match well with θ_1, and there were two transient noise periods, one at the beginning of the estimates and one at the end. Figure 4-28 show the estimates of M_α for Test Case 2 compared to the original estimates, θ_1. The overall trend was good. The original estimate is noisier than the new estimate.

Overall, results obtained for M_α were better with the band-limited white noise command

signal input than the pitch doublet.

4.5.1.2 M_q, Pitch angular acceleration per unit pitch rate:

Figure 4-29 shows the estimates, θ_2 of M_q for Test Case 1 compared to the

original estimates, θ_1. The new estimate has some transient noise at the beginning and

the end of the time history, but in the middle compares better. These erratic data points

causing the transient noise in the estimates are cause by an ill-condition X matrix for the

estimates at this time section. This will be further discussed later in this report. Figure 4-

30 shows the estimates, θ_2 of M_q for Test Case 2 compared to the original estimates, θ_1.

Other than the short transient noise occurring at the beginning of the data, the overall

trend of the new estimate follows the original estimate very well. Surprisingly, the

estimates made for M_q for both Test Cases were much better than were the original

estimates to the truth data.

4.5.1.3 $M_{\delta e}$, Pitch angular acceleration per unit elevator (pitch deflection) input:

Figure 4-31 shows the estimates, θ_2 of $M_{\delta e}$ for Test Case 1 compared to the

original estimates, θ_1. Once again, there are the transient noise caused by erratic data in

the beginning and the end of the time history of estimates. This phenomenon will be

discussed in Section 4.5.1.4.

Figure 4-32 shows the estimates, θ_2 of $M_{\delta e}$ for Test Case 2 compared to the

original estimates, θ_1. While there is some bias between the estimates, this is one of the

best matching comparisons. The bias is caused by the second order filter used to smooth

the estimate data, see Section 4.4.1.3. The trend is identical between both estimates as

are any fluctuations in the data. Overall, once again, the results obtained for $M_{\delta e}$ were

better with the band-limited white noise command signal input than the pitch doublet.

This next section will present the condition number analysis made for the Linear

Regression Validation experiment.

4.5.1.4 Condition number of Regressor Matrix, X₂

The definition of the condition number of the matrix was originally defined in

Section 4.4.1.4. Figures 4-25 and 4-26 give the condition number of the estimates, θ_2 for

the regressor matrix, X_2 for both Test Case 1 and Test Case 2. The highest and lowest

condition numbers for both commanded signal input types for X_2 are shown in Table 4-3

below.

Table 4-3: Comparison of Maximum and Minimum Condition Numbers for X_2

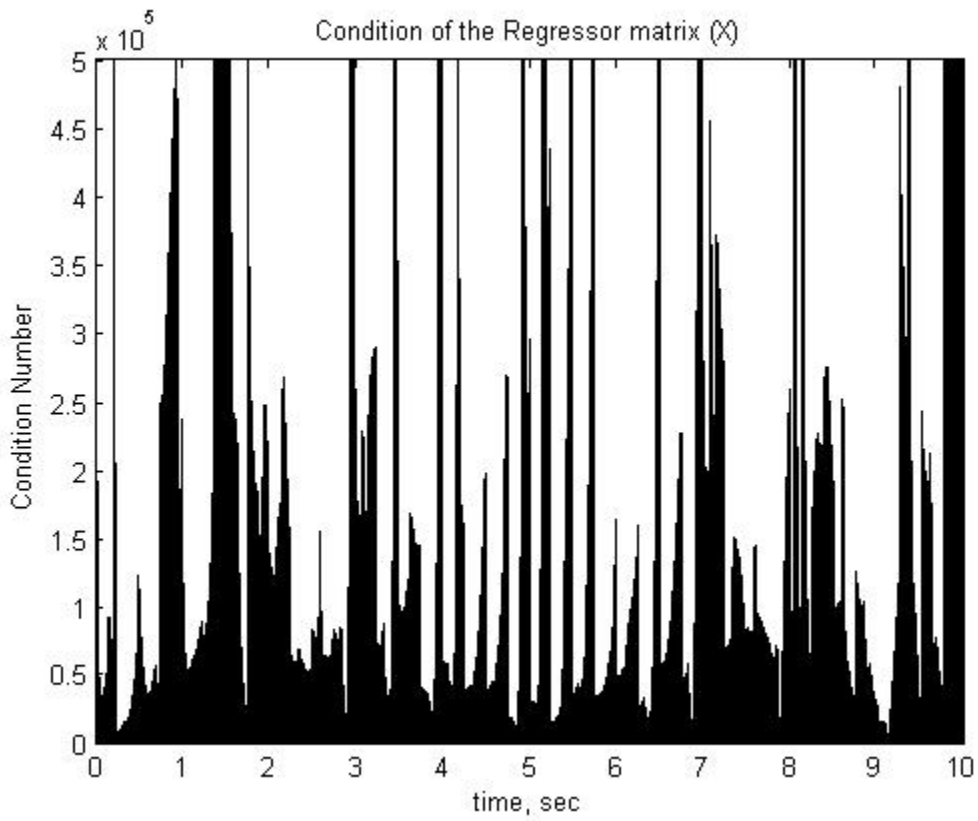| Regressor Matrix, X_2	Highest Condition Number	Lowest Condition Number
Test Case 1	$7e^9$	$11e^3$
Test Case 2	$6e^7$	40

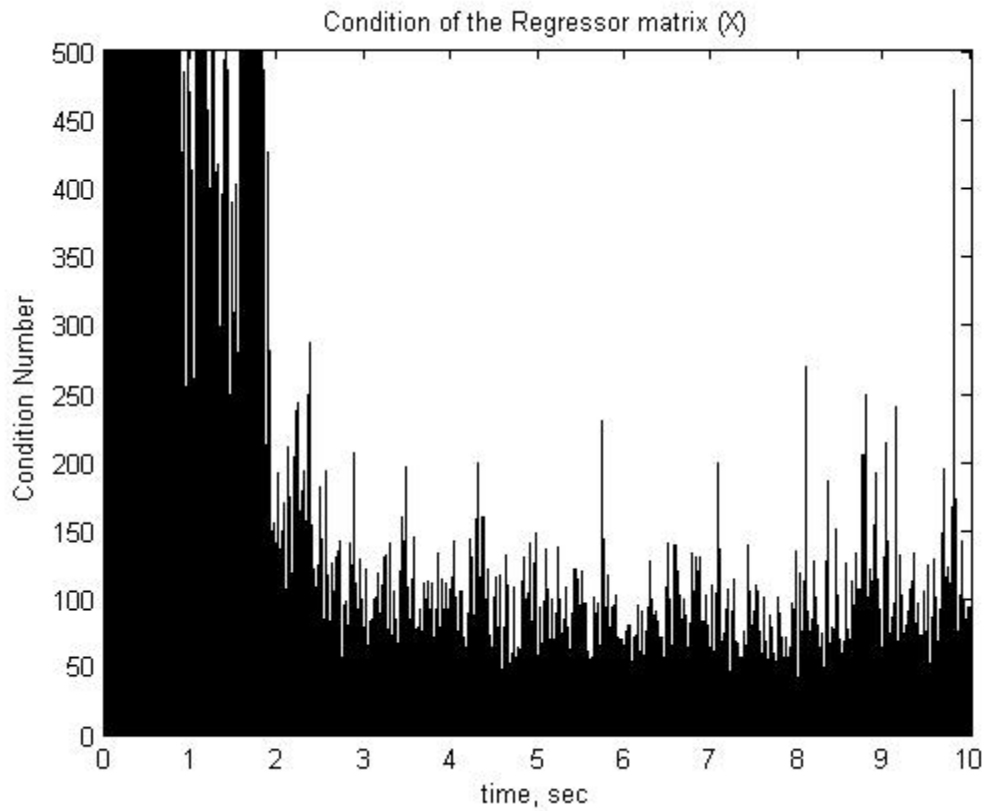**Figure 4-25 Condition Number of X_2 for Test Case 1**

Figure 4-26 Condition Number of X_2 for Test Case 2

From observation of Figure 4-25, high condition numbers occur at the beginning and the end of the time history data set similar to Figure 4-26. This again has a direct correlation to the shape of the estimates of M_α, M_q and $M_{\delta e}$ for Test Case 1 in Figures 4-27, 4-29 and 4-31, where the erratic data points in the beginning and end of the time history exist. This is another indication that the pitch doublet signal used for Test Case 1 was not set to a high enough frequency to excite all the modes of the system, which therefore, produces the singularities in the Regressor Matrix, X.

Figure 4-26 shows a large concentration of high condition numbers at the beginning of the time history data. This trend directly correlates to the cause of the large transient noise data points seen in the beginning of Figures 4-28, and 4-30 for the estimates for Test Case 2. From Figures 4-8, 4-9, 4-25 and 4-26, it is clear that the band-limited white noise signal does a better job of exciting the modes of the system than the pitch doublet due to the lower condition numbers (fewer singularities).

Generally the results of θ_2 (the longitudinal derivatives estimated from the linear model of the θ_1 estimates), proved to be an acceptable validation of the linear regression technique.
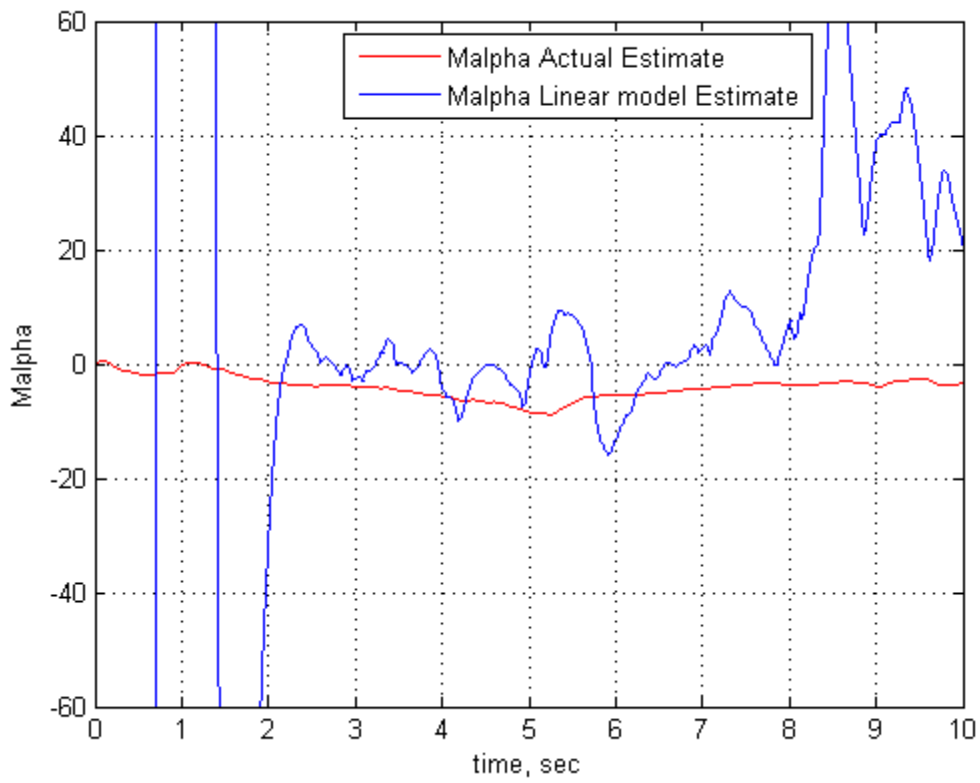
Figure 4-27 Test Case 1 Comparison of θ_1 to θ_2 for M_α
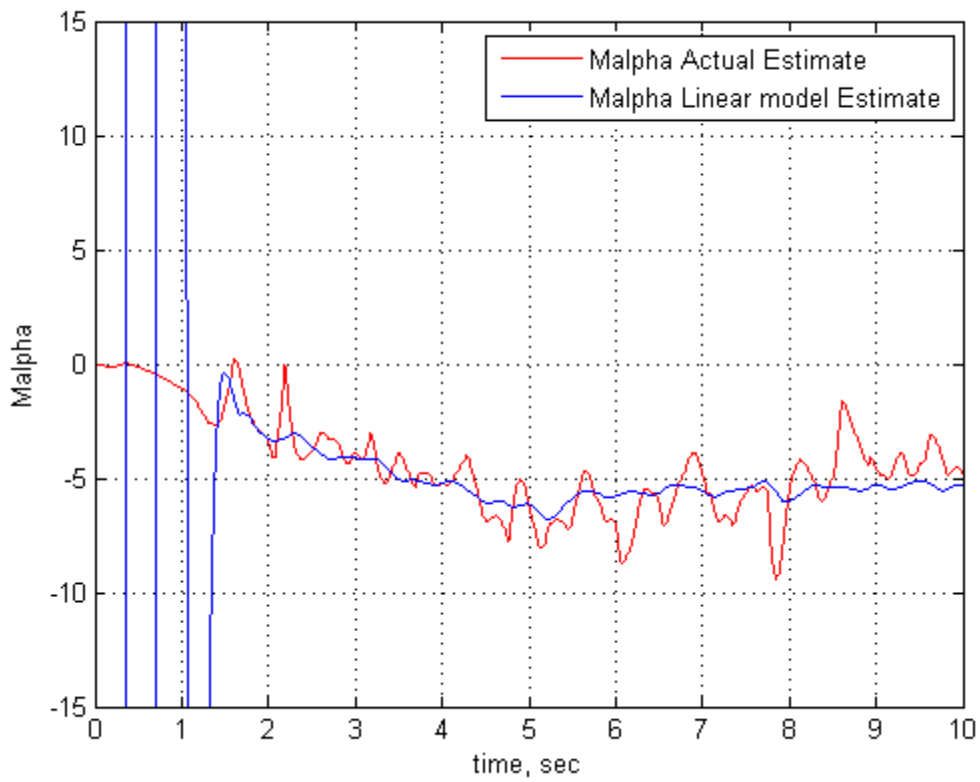

Figure 4-28 Test Case 2 Comparison of θ_1 to θ_2 for M_α
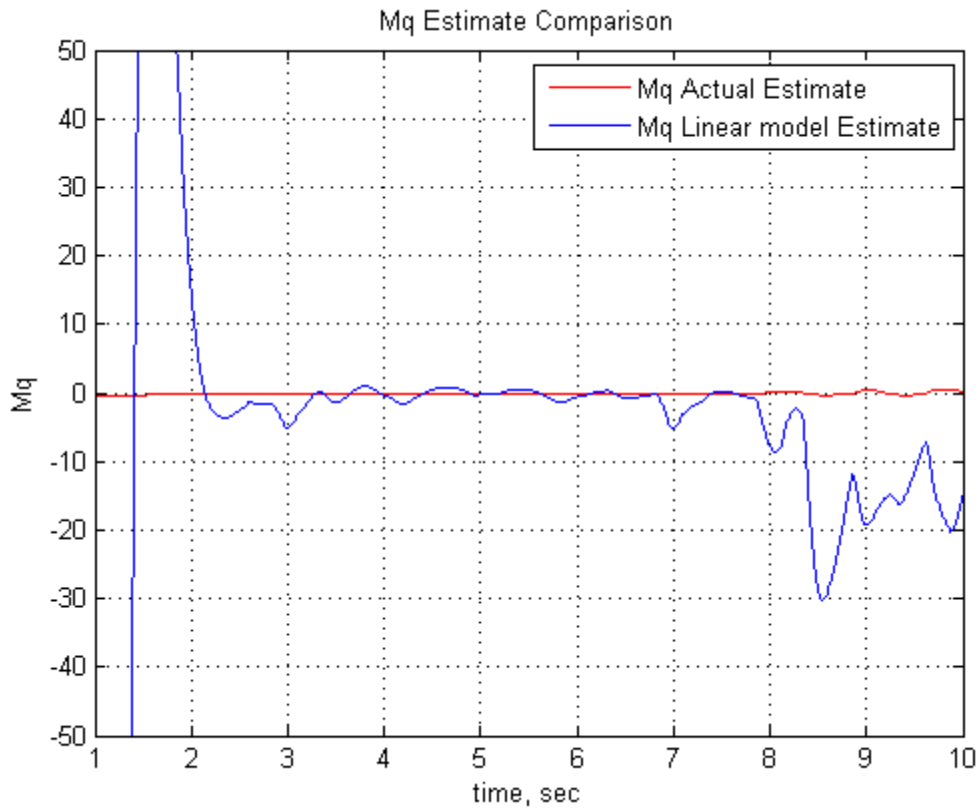
Figure 4-29 Test Case 1 Comparison of θ_1 to θ_2 for M_q
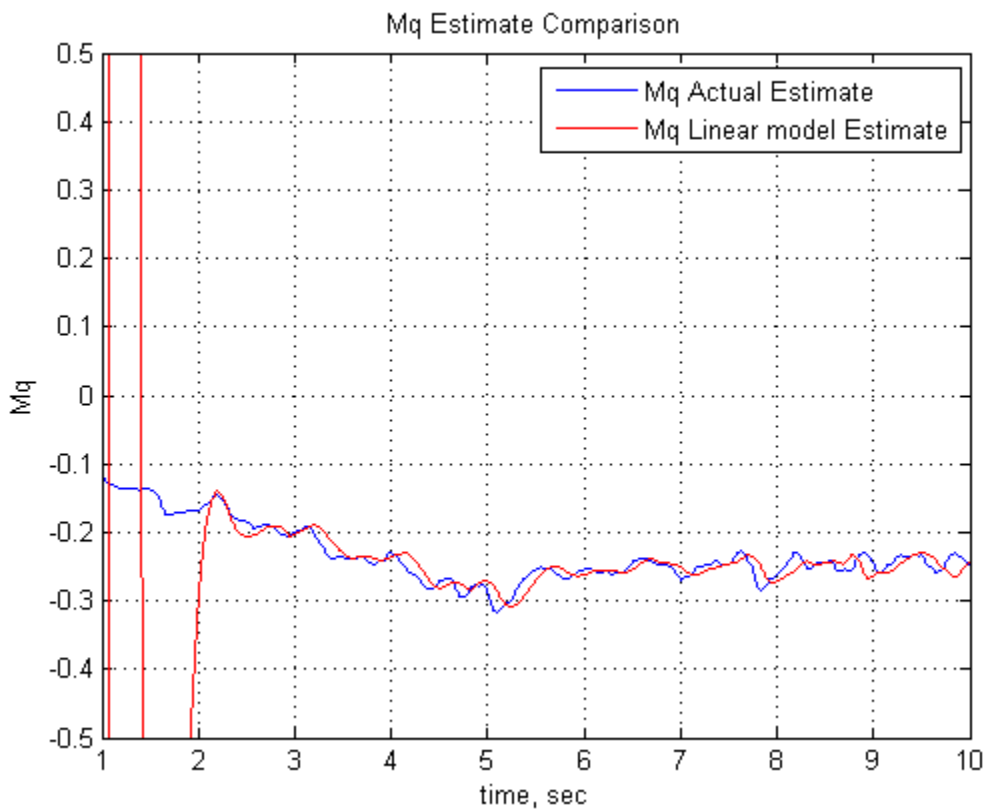
Figure 4-30 Test Case 2 Comparison of θ_1 to θ_2 for M_q
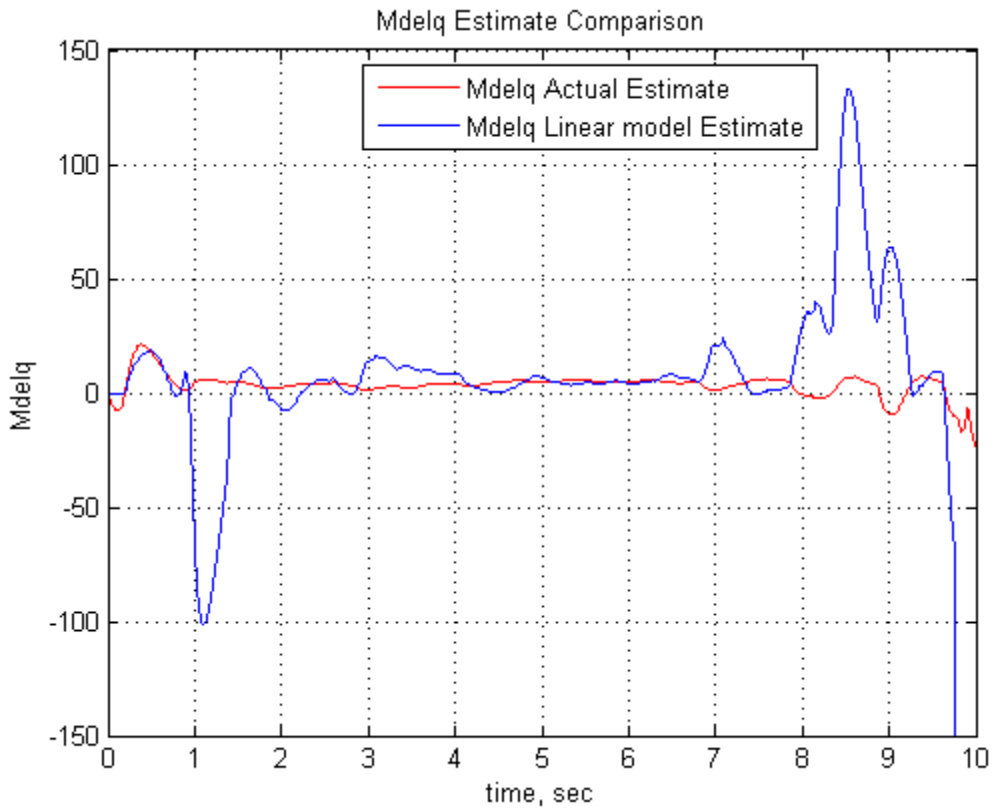
Figure 4-31 Test Case 1 Comparison of θ_1 to θ_2 for $M_{\delta e}$
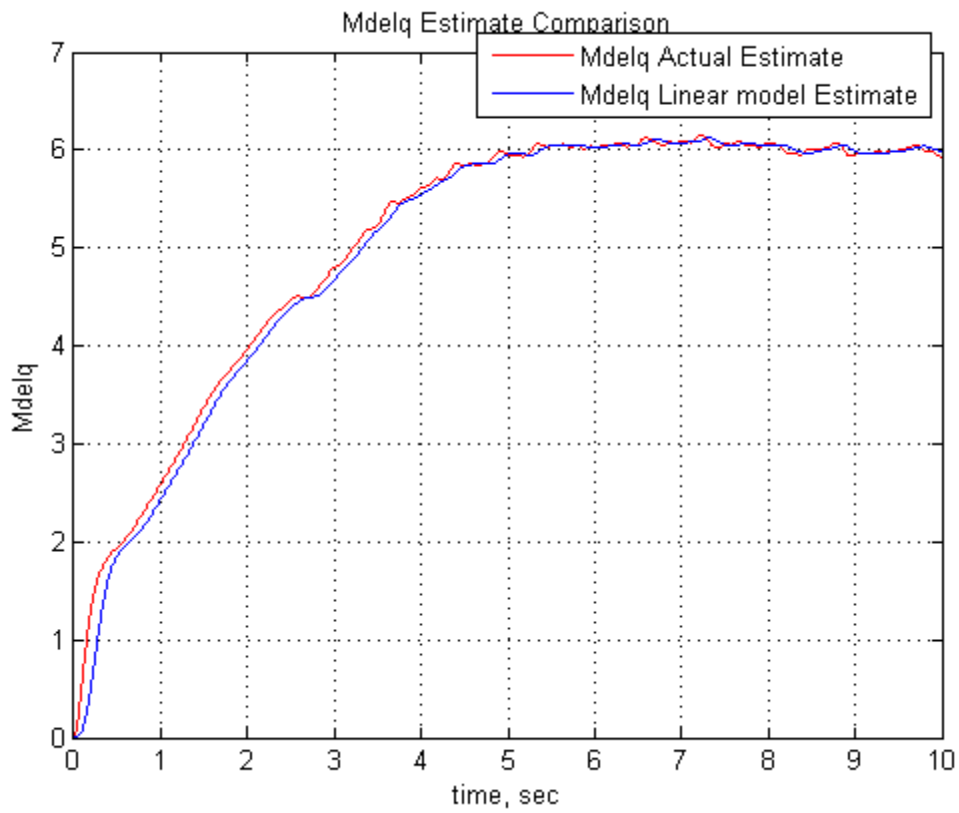
Figure 4-32 Test Case 2 Comparison of θ_1 to θ_2 for $M_{\delta e}$

5. Conclusions and Recommendations

5.1 Conclusions

Using Linear Regression as a parameter identification method to determine the longitudinal dimensional stability derivatives of a tactical missile was presented in this document. The linear regression technique was applied and compared to actual simulation data to determine the suitability of the method. Two control input forms were tested and compared. Estimates were determined from flight test data obtained from a 6-DoF missile model simulation and also from a discrete linear model of the system.

This research shows that a relatively simple estimation method such as linear regression can be used successfully in determining longitudinal dimensional stability derivatives of a tactical missile in flight. Comparative results presented in the previous section confirm that using a control input form with higher frequency modulations, such as band-limited or filtered white noise, leads to good estimates of model parameters. While this method is not as complex as other methods of parameter estimation, the results show that satisfactory estimates can be obtained in a short amount of time. This could be beneficial for engineers who require a rough estimation of missile aerodynamic parameters. The results of the research presented here will help shed light on and further the study of parameter identification for air-to-air missiles.

5.2 Recommendations Further Research

The linear regression method presented here was only applied to determining the longitudinal dimensional stability derivatives of the missile simulation. There is a need,

however, to expand this research to include the lateral-directional dimensional stability derivatives as well.

Future work should also include improving the missile simulation used in this research. The missile simulation did not include an actuator model for the control surfaces of the missile. This factor could significantly alter the results of this research. This research only concentrated on data input control signals that were not filtered by actuator dynamics. The actuator model might introduce physical limitations to the input signal, which, for example, could limit the magnitude and frequency of the input signals that were used in this research. As stated earlier, the input form should be within the bandwidth of the actuator driving the control surface being commanded for the maneuver of the missile. This factor might make using band-limited white noise or high frequency pitch doublets as input signals unfeasible for air-to-air missile parameter identification.

Expanding the experimental factors used in this research should be investigated. For this research, only two forms of control signal actuation were examined. More control signal input types, such as sinusoidal inputs or chirp signals varying in frequency would be of value to further the knowledge on this subject to the community. Different sample sizes should also be explored. For the linear regression analysis, samples of the time history data sets were limited to only 10 samples per iteration, or every 0.01 seconds for the entire time of the simulation, which ran for 10 seconds with 10,000 samples taken. The best estimates resulting from this research were for the derivatives, M_α and $M_{\delta e}$. Further research needs to be done to determine better estimates of M_q. With these recommendations for further research to be explored; a better conclusion can be made on

the applicability of using Linear Regression analysis for tactical missile aerodynamic

parameter estimation.

Bibliography

1.   Kain, James E., Charles M. Brown Jr., and Jang G. Lee. *Missile Aerodynamic Parameter and Structure Identification from Flight Test Data*. AFATL-TR-77-129. The Analytic Sciences Corporation, 1977.

2.   Mealy, Gregory L. and Arwen M. Warlock. *Airframe Coefficient Estimation System (ACES): Algorithm Manual.* TR-8977-14-2. TASC, 30 September 1999.

3.   Buffington, J., P. Chandler, M. Pachter. "Integration of On-line System Identification and Optimization-based Control Allocation," *American Institute of Aeronautics and Astronautics.* AIAA-98-4487, 1998.

4.   Smith, L., P.R. Chandler, M. Pachter. "Regularization Techniques for Real-Time Identification of Aircraft Parameters," *American Institute of Aeronautics and Astronautics.* AIAA-97-3740, 1997.

5.   Hsia, T.C. *System Identification: Least-Squares Methods.* Lexington MA: Lexington Books, 1977.

6.   Byram, Timothy R., *Final Report on High Fidelity Missile Fly Out Modeling Process Enhancement.* TAG 31-01,Contract F33657-94-D-0012. BATTELLE, October 13, 1997.

7.   Zipfel, Peter H. *Modeling and Simulation of Aerospace Vehicle Dynamics.* Reston VA: American Institute of Aeronautics and Astronautics, Inc., 2000.

8.   Roskam, Jan. *Airplane Flight Dynamics and Automatic Flight Controls.* Lawrence KS: Design, Analysis and Research Corporation (DARcorporation), 2003.

9.   Klein, Vladislav. "Estimation of Aircraft Aerodynamic Parameters from Flight Data," *Prog. Aerospace Sci.*, Vol. 26, pp. 1-77, 1989.

10.   Class notes, Mechatronics 2.737, Laboratory Assignment 6: System Identification using Frequency Response Measurements. Dept. of Mechanical Engineering, Massachusetts Institute of Technology, Cambridge, MA, 1999.

REPORT DOCUMENTATION PAGE

Form Approved
OMB No. 0704–0188

1. REPORT DATE (DD–MM–YYYY)	2. REPORT TYPE	3. DATES COVERED (From — To)
14 Sep 06	Master's Thesis	Oct 2003 — Aug 2006

4. TITLE AND SUBTITLE	5a. CONTRACT NUMBER
Parameter Estimation of a Tactical Missile using Linear Regression	5b. GRANT NUMBER
	5c. PROGRAM ELEMENT NUMBER
6. AUTHOR(S)	5d. PROJECT NUMBER
Kelly S. Powers	5e. TASK NUMBER
	5f. WORK UNIT NUMBER

7. PERFORMING ORGANIZATION NAME(S) AND ADDRESS(ES)	8. PERFORMING ORGANIZATION REPORT NUMBER
Air Force Institute of Technology Graduate School of Engineering and Management (AFIT/EN) 2950 Hobson Way WPAFB OH 45433-7765	AFIT/GAE/ENY/06-S12

9. SPONSORING / MONITORING AGENCY NAME(S) AND ADDRESS(ES)	10. SPONSOR/MONITOR'S ACRONYM(S)
James Simon NASIC/ADNW 4180 Watson Way WPAFB, OH 45433-5648	11. SPONSOR/MONITOR'S REPORT NUMBER(S)

12. DISTRIBUTION / AVAILABILITY STATEMENT

APPROVED FOR PUBLIC RELEASE; DISTRIBUTION UNLIMITED

13. SUPPLEMENTARY NOTES

14. ABSTRACT

This research presents the method of Linear Regression as a parameter identification method to determine the longitudinal dimensional stability derivatives of a tactical missile. Missile flight histories are characterized by rapid accelerations, rapidly changing mass property characteristics with often short flight times. These characteristics make accurate parameter estimation of the missile aerodynamics more challenging than for aircraft. The simulation used for this research was created in MATLAB/SIMULINK based on the missile trajectory program, TRAP. The aerodynamic data for the 6-DoF missile model was based on a supersonic, tail controlled missile similar to an AIM-9X missile. Two command input types were investigated for excitation of the system modes.
This research shows that linear regression can be used successfully in determining longitudinal dimensional stability derivatives of a tactical missile in flight when using a control input form with higher frequency modulations, such as band-limited or filtered white noise.

15. SUBJECT TERMS

Tactical Missiles, Aerodynamics, Linear Regression, Parameter Estimation, Longitudinal Stability coefficients, Modeling and Simulation, MATLAB/SIMULINK.

16. SECURITY CLASSIFICATION OF:			17. LIMITATION OF ABSTRACT	18. NUMBER OF PAGES	19a. NAME OF RESPONSIBLE PERSON
a. REPORT	b. ABSTRACT	c. THIS PAGE	UU	97	Dr. David R. Jacques
U	U	U			19b. TELEPHONE NUMBER (Include Area Code) (937) 255-3355, ext 3329; e-mail: David.Jacques@afit.edu

Standard Form 298 (Rev. 8–98)
Prescribed by ANSI Std. Z39.18